AD-A055 687 AIR FORCE INST OF TECH WRIGHT-PATTERSON AFB OHIO SCH--ETC F/G 9/2
THE STATIC CHARACTERIZATION OF MAGNETIC BUBBLE FILMS USING SPAT--ETC(U)
DEC 77 R A MCDONALD

UNCLASSIFIED AFIT/GE/EE/77-27

1 OF 2
AD A055 687

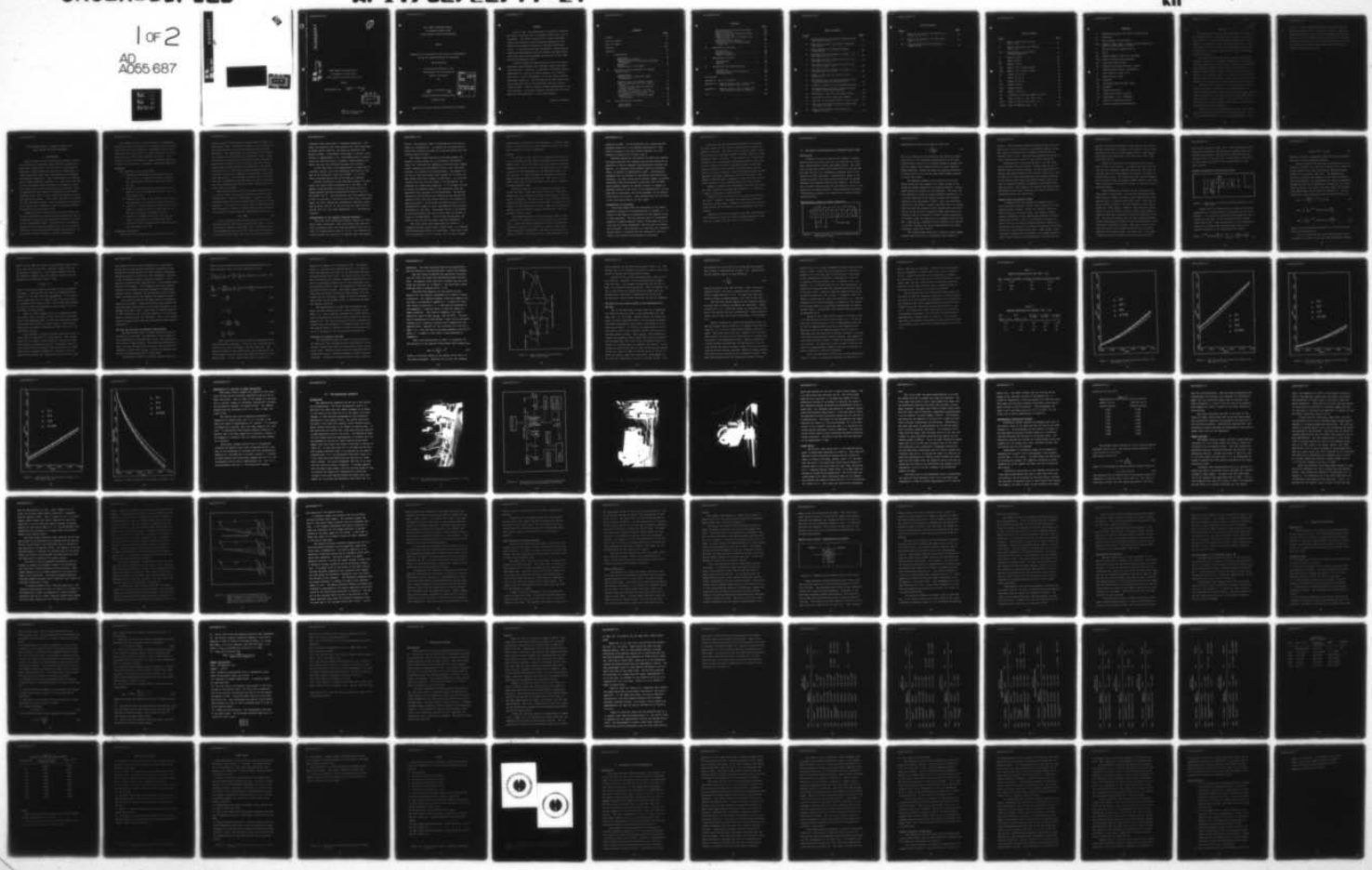

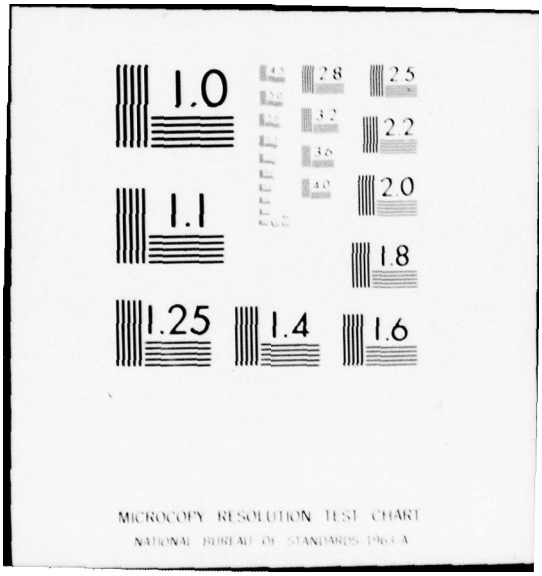
1.0
1.1
1.25
1.4
1.6
1.8
2.0
2.2
2.5
2.8
3.2
3.6
4.0
MICROCOPY RESOLUTION TEST CHART
NATIONAL BUREAU OF STANDARDS 1963-A

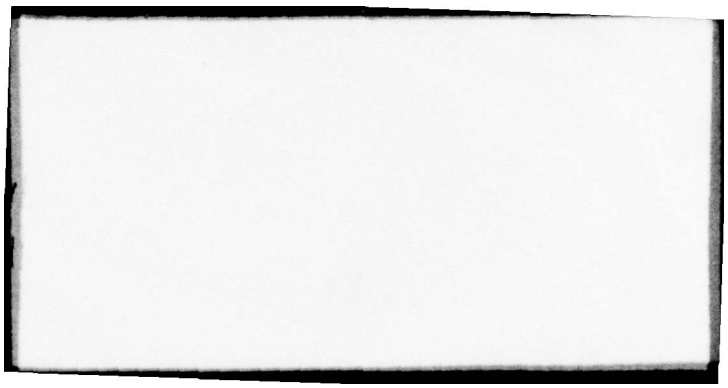

AFIT/GE/EE/77-27

THE STATIC CHARACTERIZATION OF MAGNETIC BUBBLE FILMS USING SPATIAL FILTERING TECHNIQUES

THESIS

Robert A. McDonald
Capt USAF

AFIT/GE/EE/77-27

AFIT/GE/EE/77-27

THE STATIC CHARACTERIZATION OF MAGNETIC BUBBLE FILMS USING SPATIAL FILTERING TECHNIQUES

THESIS

Presented to the Faculty of the School of Engineering

of the Air Force Institute of Technology

Air University

in Partial Fulfillment of the

Requirements for the Degree of

Master of Science

by

Robert A. McDonald, B.S.
Capt USAF

Graduate Electrical Engineering

December 1977

Approved for public release; distribution unlimited.

Preface

In this study, the performance of a system to evaluate the static characteristics of magnetic bubble films was investigated. The system consisted of a laser-illuminated sample and diffraction angle measuring apparatus in conjunction with spatial filtering of unwanted diffraction orders. It was determined that stripewidth, characteristic length and magnetization could be measured but that significant difference existed between the results of this study and the manufacturer's data.

I wish to express my appreciation to the following individuals, whose guidance and technical support made this study possible: Professor J. Lubelfeld, my faculty advisor; Capt Robert E. Johnson, my thesis sponsor; Dr. Millard G. Mier and Mr. John M. Blasingame, of the Air Force Avionics Laboratory (AFAL); Mr. Jack Tiffany of the AFIT school shop who constructed some of the apparatus; and Maj. Clark W. Searle, USAFR. I wish to express special appreciation to my wife, Barbara. It was her devotion, patience and toil that made the AFIT experience so rich and rewarding.

Robert A. McDonald

Contents

Contents

List of Figures

List of Figures

List of Tables

Notation

α	absorption constant for light in Garnet films
cm	centimeter
D	stripe period in micrometers
D_{FF}	magnetic bubble film - spatial filter distance in inches or centimeters as noted
F	Faraday rotation, degrees per cm
G	Gauss
HA	applied magnetic field, DC, Oersteds
Hcol	bubble collapse field, Oersteds
Hk	anistropic field, Gauss
Ku	uniaxial anisotropy constant, erg/cm^2
L	characteristic length, micrometers
λ	wave length of laser in um
M	magnetization, Gauss
mw	milliwatt
M_S	saturation magnetization, Gauss
Oe	Oersteds
sd	Standard Deviation
σ_w	domain wall energy, erg/cm^2
um	micrometer, 1 um = 10^{-6}meters
V	mobility, cm/second-Oersted
W	domain stripewidth, micrometers

Abstract

The primary objectives of this study were to confirm the spatial filtering technique for the static characterization of 4 to 7 um stripewidth magnetic bubble films, and to extend the technique to 1 to 3 um stripewidth films. Also an objective was to determine the uncertainty in $4\pi M_s$ value if infinite Q is assumed, when in fact a more modest value ($3<Q<5$) is present.

The spatial filtering technique used the diffraction grating properties of a magnetic bubble film in conjunction with the equations of Kooy and Enz to determine stripewidth, characteristic length, and saturation magnetization. The spatial filter removes unwanted orders from the diffraction pattern. The filtered signal is focused on a photodetector and the first order diffraction angle measured to find stripewidth and the second order to find saturation magnetization.

The Kooy and Enz equation were computer programmed and tables and plots of characteristic length/thickness and applied field/saturation magnetization prepared. The Quality factor dependence of the equations was investigated and it is shown that for a Quality factor of 3, and a domain period/thickness of 0.7, a 14 percent uncertainty in the saturation magnetization could be incurred.

The results of the experimental portion of this study do not confirm the spatial filtering technique for 4 to 7 um films nor extend it to 1 to 3 um stripewidth films. Of 20

trials to measure stripewidth in 4 to 7 um films only 12 were within 10 percent of manufacturer's data. Saturation magnetization values were up to ± 50 percent of manufacturer's data. It is considered possible that lack of suitable magnetic preconditioning before taking measurements contributed to the discrepancy between data obtained from this study and manufacturer's data.

THE CHARACTERIZATION OF MAGNETIC BUBBLE FILMS USING SPATIAL FILTERING TECHNIQUES

I. Introduction

Magnetic bubble digital storage and processing systems are one method of obtaining large (10^{12}) bit capacity computer data storage units. The Air Force is interested in obtaining a large computer system with no moving parts, extreme reliability, small size, lightweight, and stringent environmental capability. These requirements are currently met by rugged mechanical systems, i.e., disk, drum, and tape. One use of magnetic bubble memories is to replace a satellite digital tape recorder that must have zero power standby requirements; high untended reliability; environmental capabilities of -25°C to +75°C; radiation-hardness; and minimal gyroscopic effects. Data access time can be in seconds for this type mass storage. These requirements are expected to be ideally met by magnetic bubble, mass-storage devices featuring block access (Ref 2:1-2).

Magnetic bubble technology today does not satisfy all of the requirements for spacecraft and airborne use, but the technology is young and new materials for devices are still in the developmental stage. Currently 4 to 6 um diameter bubbles are the industry standard, but 2 to 3 um bubble materials are being actively investigated (Ref 5:12/1-1), and even smaller bubble diameters are being contemplated.

The material used for current devices is liquid-phase epitaxially grown garnet film on a gadolinium gallium garnet (3 G) substrate. (Ref 5:12/1-1). Characterization of these garnet films for device use is of prime importance to better understand and utilize these materials in devices. Also testing and defect detection for sample and production runs of device grade material is becoming increasingly important.

Objectives

The objectives of this study were:

1. Confirm the technique for static characterization of Dr. R. D. Henry using spatial filtering of a bubble-film diffracted laser beam (Ref 10, 11, 12).
2. Extend the spatial filtering technique from the present 4 to 6 um stripewidth films to 1 to 3 um stripewidth films.
3. Determine the effect of the Quality factor (Q) on the measurement of saturation magnetization (Ms).
4. Determine if any magnetic pre-conditioning of the sample is required and if so, what type yields the most consistent, repeatable results.
5. Determine if single-sided films yield the same static characteristics as double-sided films.
6. Determine if the technique can be used to measure the anisotropy field, Hk.

Background Information

Polarization microscopy and spectrophotometry are the

present means of characterizing magnetic bubble domains in thin garnet films. The static properties of the domains are determined by measuring the film thickness (H) by spectrophotometry. The stripewidth (W), and collapse field (Hcol) are measured by polarization microscopy (Ref 7:192). These measurements are applied to theoretical models developed by Kooy and Enz (1960), (Ref 15) or Thiele (Ref 22), and the static bubble characteristics are calculated. The static characteristics of interest in device manufacture are: characteristic length (L), saturation magnetization, and domain wall energy (σ_w). The anisotropy constant (Ku) is obtained from the susceptibility measured using an optical magnetometer, and coercivity (Hc) from the stripe domain response to an AC field (Ref 7:191).

The characterization of films is important because it is from the static and dynamic properties of bubbles that suitability for devices is determined. Results of static characterization are used in several ways by the device manufacturer. For example, to prevent the self-demagnetization and the spurious creation of bubble domains, the nucleation field should be larger than the demagnetizing field, i.e.,

$$Hk > 4\pi M_s \qquad (1)$$

In the primarily optical processes used to date for characterization, there are several problem areas. In the first place, moderate-sized bubble (4 to 7 um) devices are in the production stage, and since each film grown requires a characterization check, the cost of having a skilled mi-

croscopist check each wafer is becoming significant. Secondly, new materials are being explored for their usefulness as bubble domain memories, and these new materials have smaller bubbles. Polarization microscopy is limited in resolution to approximately 1 um. New methods must be found to obtain the characteristics of magnetic bubble materials as bubble size and film thickness decrease (Ref 10:1285).

In CGS units $4\pi M_s$ is the magnetization in Gauss and in a perfect crystal, Hk is the anisotropy field which is the same as the nucleation field (Ref 13:169). It is from static characterization that Hk and $4\pi M_s$ are obtained.

Spatial filtering is a new technique proposed for measuring the static bubble parameters of W, and $4\pi M_s$. The spatial filtering method conceives the bubble film as a binary magnetic grating as described by Mezrich (Ref 17) and Haskel (Ref 8). The information about the magnetic properties is contained in the first and second order diffracted beams, and after appropriate mathematical treatment, developed by Henry (Ref 10, 11, and 12) from the theory of Kooy and Enz (Ref 15), the static parameters, W, L, and $4\pi M_s$ are obtained.

Implementation of the Spatial Filtering Technique

The first order diffraction pattern contains the information about stripewidth, while the second order beam contains information about $4\pi M_s$ when the applied field, Hk results in a magnetization equal to 1/2 M_s. The unwanted diffraction orders are removed by an annular pass-ring spatial

filter. The resultant light is collected by a lens and focused on a photodetector. In essence one is measuring the first order diffraction angle for W and the second order diffraction angle for $4\pi M_s$.

The optical setup required for the measurements consisted, in final design, as a 15 milliwatt, Helium-Neon Laser, coil structure for applying a DC and AC field, sample holder, annular pass-ring spatial filter, lens, and photodetector, all mounted on an optical bench. The spatial filter was an aluminized glass slide (except for a 0.6326 inch mean radius ring with a width of 0.030 inch). If an AC modulating field was used the output of the photodiode was connected to a phase-lock amplifier. If DC voltage was used to locate the maximum output of the photodiode, then the photodiode was connected to a microvoltmeter. The maximum response of the photodiode was obtained by positioning the spatial filter along the optical bench and the diffraction angle calculated. The Kooy and Enz model was used to find characteristic length (L) and a new spatial filter position calculated to find $4\pi M_s$. The spatial filter is positioned at this new position and the DC field swept for maximum response of the photodiode. The DC field was measured, applied to the Kooy and Enz model, and $4\pi M_s$ determined.

The films chosen were manufactured by various U. S. companies and were single layer, double sided, 1 in diameter films epitaxially grown on 3G substrates. Films with a zero field stripewidth of 4 to 7 um and 1 to 3 um were cleaned,

mounted and characterized in the apparatus. One film, number 1-9-3, was cleaned, and one side etched away until the sample was a single-sided film on substrate.

Results

The results of the study do not confirm the spatial filtering technique for the static characterization of magnetic bubble films. Out of 20 trials using the spatial filtering apparatus to measure W in 4 to 7 um films only 3 were within 1 percent of the manufacturer's data and these three were for one film. Of the 20 trials, 12 deviated less than 10 percent from the manufacturer's data. For the 1 to 3 um films tested only 3 out of 12 trials were within 5 percent of manufacturer's data.

The $4\pi M_s$ value for 4 to 7 um films was measured in 9 trials and only 1 trial was within 10 percent. The other measurements show deviation from the manufacturer's data of up to -51 percent. Only two of the 1 to 3 um films could be tested for $4\pi M_s$ and the values range from + 1 percent to + 61 percent of the manufacturer's data. There was no systematic pattern to the difference between manufacturer's data and spatial filtering data.

The theoretical part of the study showed that if $4\pi M_s$ is desired to 1 percent for 1 to 3 um films then Q dependence in the Kooy and Enz equations must be accounted for. Industrial practice is to treat Q as infinite when using these equations, measure $4\pi M_s$, and then measure the anisotropic field Hk. An estimate of Q is then obtained by di-

viding Hk by $4\pi M_s$. It was found that for a domain period/thickness (D/H) of 0.7 a 14 percent uncertainty in $4\pi M_s$ would be induced in the Kooy and Enz equation if Q were treated as infinite but in fact Q was 3.

Possible reasons for the failure to confirm the spatial filtering technique were examined and the most plausible explanation is that an improper preconditioning technique was applied. No technique tried yielded results consistently within 10 percent of manufacturer's data. Unfortunately, equipment was not available to try Henry's preconditioning technique. He used a slow (10 sec period) ramped, sinusoidal saturating field electronically controlled (Ref 12:1529). Other possible reasons for failure include: 1) magnetic or physical defects in the films, 2) the manufacturers' optical data may be inaccurate, and 3) the passband of the spatial filter may be too narrow. These possibilities are discussed in the Conclusions section of this report.

Presentation of the Report

This study begins with the description of the static parameters required for characterization in Chapter II. An outline of the theory of diffraction by thin magnetic films is also presented. The Kooy and Enz model for stripewidth response to applied magnetic fields is discussed and it is shown how the static parameters W and $4\pi M_s$ may be obtained from the model. The constraint on W and $4\pi M_s$ with regard to quality factor is analyzed and the technique of using infinite Q for practical measurements is discussed.

In Chapter III the experimental apparatus is described in detail along with the various setups used in attempts to measure W and $4\pi M_s$. The laser light source and signal detection equipment is discussed and the different types of signal detection schemes presented. This chapter also includes the technique used to photograph diffraction patterns which were used to confirm that usable information exists in the diffraction patterns and to explain possible reasons why the results are not as expected. The construction details of the apparatus and sample preparation are also discussed. This chapter concludes with a discussion of the physical measurements required and the expected precision of the results.

Chapter IV details the experimental procedure and lists the steps required to measure and calculate W, L, and $4\pi M_s$. A sample calculation is also provided.

Chapter V lists the results in 11 tables and describes the films. Chapter VI presents the conclusions and recommendations of the study. Chapter VI also discusses the possible sources of discrepancy in the measurements and calculations.

Appendix A lists the equipment used with specifications, while Appendix B gives the Fortran computer program for HA/$4\pi M_s$ and a sample from the table is also provided.

II. The Static Characterization of Magnetic Bubble Films

Introduction

A number of factors influence the design of magnetic bubble devices but three that are very important are thickness, characteristic length, and magnetization. The thickness is important because both Thiele (Ref 22) and Kooy and Enz (Ref 15) use H as a fundamental boundary value in the solution of their equations. Characteristic length is important because it is used in the determination of optimum thickness and probable stable bubble diameter. Magnetization is used in several ways but one important way is in the prediction of bubble velocity. These analytical and device considerations emphasize the importance of static material characterization.

Characteristic Length and Domain Dimensions

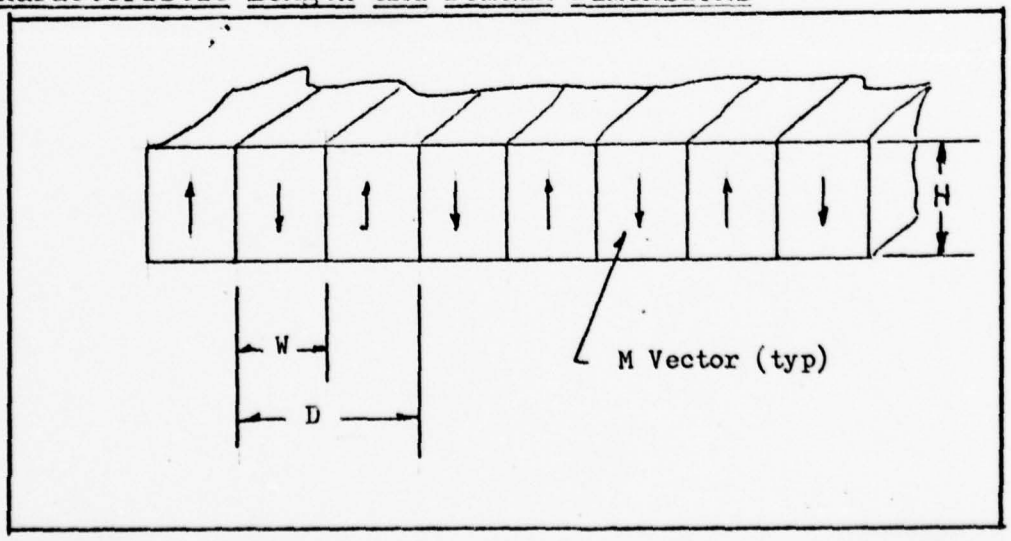

Figure 1. Stripe Domains of Alternating Magnetization, Zero Applied Field

Characteristic length is defined as (Ref 1:24)

$$L = \frac{\sigma_w}{4\pi M_s^2} \qquad (2)$$

Here σ_w is defined as the energy per unit area of a domain wall and M_s is the saturation magnetization in CGS units. Characteristic length is of interest because it governs the scale of domain sizes characteristic of a given magnetic bubble material. Thiele has shown the optimum thickness of a bubble film to be 4L and the mean stable bubble diameter to be 8L (Ref 7:170).

The approach commonly in use today is to use the Thiele theory for the diameter of a bubble either at the stripe to bubble transition or at bubble collapse. Several difficulties are inherent in this approach. The first and most important is that as bubble diameters decrease to 1 to 3 um the resolution of the bubble collapse field becomes limited by the wavelength of light. Also, the observable accuracy of the stripe to bubble transition point is limited both by coercivity effects in real samples and by the ability of the eye to detect changes in small noncircular distortions, that is, the point at which a stripe transitions to a bubble under the influence of an applied field (Ref 20: 56). Shaw, et al., maintain that an accuracy of ±7 percent is the best possible for optical measurements from bubble transition states (Ref 20:57).

The normal domain period for a magnetic bubble sample in zero applied field is a serpentine array similar to

Figure 1. The alternate regions of magnetization will have equal width in order to yield a net magnetic moment of zero. The width is a function only of sample thickness and the characteristic length. Kooy and Enz developed the theory relating characteristic length to zero field stripewidth.

Experimentally, the domain period, D, at zero field can be measured with much greater accuracy than can an individual domain diameter because: 1) the stripe period is greater than bubble diameter by at least a factor of 2, and 2) effects of finite coercivity are more readily minimized in the stripe pattern than for bubbles because there is no fear of collapsing bubbles by applying a pre-conditioning magnetic field. Shaw, et al., recommended the stripe domain measurement as the most convenient and accurate method for the determination of L (Ref 20:65).

Magnetization and Magnetic Fields

A common method of measuring the magnetization of a thin optically transparent bubble domain samples is to use magneto-optical methods. Either the theory of Thiele or that of Kooy and Enz may be used. The theory of Thiele yields an equation for the equilibrium condition of bubble domains (Ref 20:70). Once L, H, and bubble diameter are known, the value of $4\pi M_s$ for high anisotropic films can be determined from graphs of the stability functions plotted by Thiele (Ref 2:44 and Ref 22:347-395). Shaw, et al., quote ±3 percent accuracy for this method, even though characteristic length can not be determined more precisely than ±7

percent, because of the nature of the equation (Ref 20:71). Another common method is based on the bubble collapse field; relating it to the zero field domain period. Shaw, et al., quote ±7 percent measurement error for $4\pi M_s$ by this technique (Ref 20:71).

Bobeck has stated that the magnetization of a film must be known to ±1 percent. He states that even with this accuracy the acceptable operating bias range (the range of external field for which bubbles are stable) is reduced 15 percent (Ref 4:251). This means also that other techniques used to measure $4\pi M_s$ not based on bubble diameter, must also have an accuracy of at least ±1 percent if they are to be of practical value.

Three methods are available for the measurement of $4\pi M_s$ based on stripewidth. All use the Kooy and Enz model which yields a formula relating period, magnetization, and quality factor to applied field (Ref 15:21). The first of these methods is based on the full hysteresis curve (M/M_s versus H). Shaw, et al., estimate that relative measurements of $4\pi M_s$ can be made within ±3 percent from sample to sample of the same composition using this technique (Ref 20: 77). The second technique involves low frequency susceptibility measurements developed by Maartense and Searle of the University of Manitoba, Canada. They do not calculate an expected accuracy but present results within ±1 percent agreement with manufacturers' data (Ref 16:6). The third technique uses the spatially filtered second order dif-

fracted beam related to $M/M_S = 0.5$. This technique uses the Kooy and Enz equation with arguments of quality factor and reduced domain period. The period is reduced because the external field is no longer zero. Henry quotes an accuracy of better than 5 percent in this determination of $4\pi M_S$ (Ref 13:1529).

Optical Properties of Thin Magnetic Films

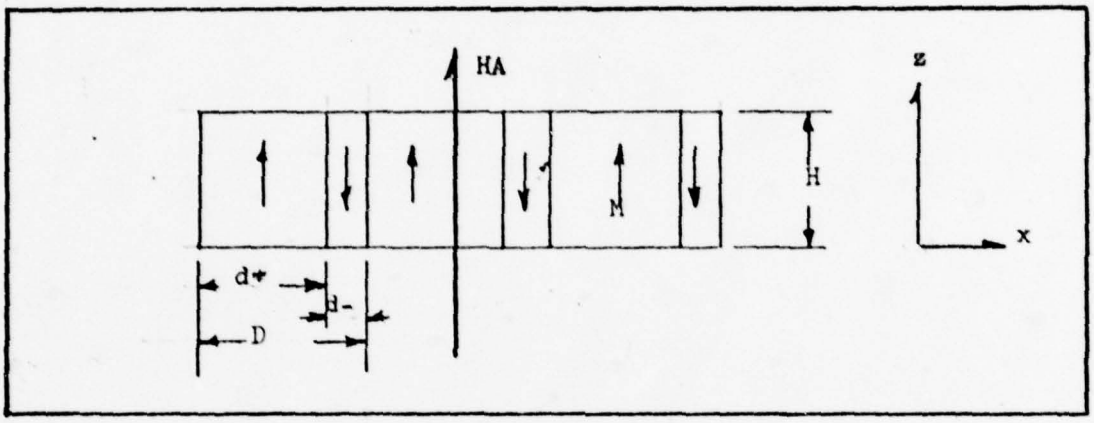

Figure 2. Edge View of Garnet Film Without Substrate (From Ref 8:542).

Haskal (Ref 8) determined that a magnetic film can be represented as a binary magnetic diffraction grating as in Figure 2. If a linearly y-polarized electromagnetic wave is incident on the film, it will be rotated by the Faraday effect (Ref 8:542). From consideration of the transmission functions and attenuation constant Haskal arrives at a Fourier expansion for the transmitted wave, giving

$$Tx(x) = e^{-\alpha H/2} \sin(FH)\left[\frac{2d_+ - D}{D} + \frac{4}{\pi}\sum_{n=1}^{\infty}\frac{1}{n}\sin\frac{\pi n d_+}{D}\cos\frac{2\pi n x}{D}\right] \qquad (3)$$

$$Ty(x)e^{-\alpha H/2}\cos(FH) \qquad (4)$$

Where Tx and Ty are transmission functions of the polarized wave and x is the absorption constant.

A garnet bubble film that has been magnetized to saturation by a normal field (HA) and returned to zero (HA=0) is a phase grating with the orientation of domains randomly placed in the x-y plane (Ref 11:1). By appropriately placing a polarizer and analyzer, or by using a polarized laser and analyzer, the y-polarized wave that is transmitted through the film can be eliminated, leaving only the x diffraction orders. For these x-polarized waves, all diffraction orders exist and are given by Equation (3). The intensities of these orders are given by Henry (Ref 7:1) as

$$Ixo = Io\left(\frac{2d_+ - D}{D}\right)e^{-\alpha H}\sin^2(FH) \qquad (5)$$

$$Ix_1 = Io\,\frac{8}{\pi^2}\,e^{-\alpha H}\sin^2(FH)\,\sin^2\left(\frac{\pi d_+}{D}\right) \qquad (6)$$

$$Ix_2 = Io\,\frac{2}{\pi^2}\,e^{-\alpha H}\sin^2(FH)\,\sin^2\left(\frac{2\pi d_+}{D}\right) \qquad (7)$$

where α is the absorption constant and F is the Faraday rotation in degrees per cm.

It can be seen from the above equations that when d+ is equal to d-, which is the case when the applied external

field is zero, then Ix1 is the only diffraction order of the first three which is present. When d± is equal to d- the stripewidth is labeled W. If the orders greater than two are removed by annular pass ring spatial filtering and one measurers the diffraction angle θ, then

$$2 W \sin \theta = \lambda \tag{8}$$

where λ is the wave length of the light used to illuminate the sample. From Equation (8) comes the fundamental measurement of W for the zero field stripewidth. It can also be seen in Equations (5), (6), and (7) that this second order is a maximum for d+ equal to D/4. This second order maximum is related to the 1/2 magnetization point ($M/M_s = 0.5$) by the theory of Kooy and Enz.

Since the actual domains exist in a serpentine array one can see there is nothing special about the x-y orientation of the impinging beam. In fact the diffraction pattern is circular when viewed in a plane normal to the incident beam due to the random orientation of small portions of the diffraction grating.

The technique of spatial filtering characterization is based upon the regularity of stripe domains. Some irregularity in the widths of stripe domains is present in films with magnetic and physical defects. Coercivity, which affects the domain wall movement, also may change the stripewidth after a magnetic disturbance. However, it was assumed for this study that stripewidths covered by the laser

beam should average out any irregularities. From photographs taken of domains by polorization microscopy in the Electronics Research Branch, Air Force Avionics Laboratory, Wright-Patterson Air Force Base, Ohio (AFAL/DHR), a maximum of ten stripewidths could be used to determine W. For a nominal 4 um stripewidth illuminated by a 1 mm diameter beam there are 125 periods. It was assumed that this ten-fold increase in the number of periods measured by diffraction analysis should compensate for the effects of local differences in coercivity and for magnetic and physical defects.

Laser beam heating of the sample was not considered a factor in this study. Askkin and Dziedzie have stated that they could move bubbles with 10 mw of power focused to 5 um diameter beam (Ref 1:336). This yields an average power of 5×10^4 watts/cm^2. The 1 mm beam diameter of a 15 mw laser yields an average power of 2 watts/cm^2. Thus it was assumed that no heating effects from the illuminating laser would be encountered.

The Kooy and Enz Model of Magnetic Bubble Domains

The Kooy and Enz model of domain theory was used extensively in this study. The equations of this theory relate stripewidth to characteristic length, and applied magnetic field to magnetization. The equations include the effects of finite anisotropy and have been used by other researchers, notably Shaw, et al., in their recommended methods for characterization (Ref 21:2346-2349).

The pertinent results of the Kooy and Enz theory are

given in two equations which have been manipulated here to make them more useful for this study (Ref 15:21).

$$\frac{L}{H} = \frac{u}{4\pi a^2} \sum_{n=1}^{\infty} \frac{1}{n^3} \sin^2 \left(\frac{n\pi}{2}\left(1+\frac{M}{M_S}\right)\right)\left[1-(1+2\pi na)\exp(-2\pi na)\right] \quad (9)$$

$$\frac{HA}{4\pi M_S} = 1+ \frac{2\sqrt{u}}{(1+\sqrt{u})\ \pi^2 a} \sum_{n=1}^{\infty} \frac{1}{n^3} \sin n\pi\left(1+\frac{M}{M_S}\right)\left[1-\exp(-2\pi na)\right] \quad (10)$$

where

$$a = \frac{H\sqrt{u}}{D} \quad (11)$$

$$u = 1+ \frac{1}{Q} \quad (12)$$

$$Q = \frac{2\ ku}{4\pi M_S^2} = \frac{Hk}{4\pi M_S} \quad (13)$$

$$\frac{M}{M_S} = \frac{d+ \ -d-}{D} \quad (14)$$

These equations are used to find the fundamental material parameters L and $4\pi M_S$. It can be seen from Equation (9) that if D, H, and Q are known, L can be calculated. The optical thickness H is measured using spectrophotometry and W is measured using the first order diffraction angle, as in Equation (8). In zero applied field M/M_S is equal to 0,

because d+ is equal to d- in Equation (14). The quality factor, Q, for devices is usually between 1 to 5 (Ref 12: 1528) and represents the ratio of the anisotropy field to the magnetization (Ref 3:47). The quality factor is difficult to determine and requires a separate measurement of either the anisotropy constant, Ku, or the anisotropy field. The anistropy field is that field required to bring the magnetization vector in-plane. The normal industry practice when using the theory of Thiele or Kooy and Enz is to initially treat Q as infinite, compute L based on infinite Q, then measure the anisotropy field, or anisotropy constant, and compute Q (Ref 27).

The magnetization is found from the Equation (10) using the same arguments as (9), except that M/M_s is now $M/M_s = 0.5$. This condition represents $d+ = (3/4)D$ which is also the maximum for the second order diffraction angle in Equation (7). The zero field period is not a constant but changes under the influence of an applied field (Ref 3:25). The quality factor is treated as infinite in Equation (10), as it is in Equation (9), for practical measurements.

Procedure For Finding W and $4\pi M_s$

The parameters chosen for study in this work were W and $4\pi M_s$ since they incorporated the calculation of characteristic length from W and the calculation of $4\pi M_s$ from applied field. Thickness values used were determined by the manufacturer since a thickness measuring facility was not available. Thickness is usually measured using a spectro-

photometer. The exact procedure used by the manufacturer and the accuracy of the manufacturers' results are unknown.

The zero field stripewidth was calculated from Equation (8) after the first order diffraction angle was measured. The spatial filter was used to ensure only the first order was selected, as in Figure 3. The zero-field stripewidth was used to compute D/H (D = 2 W).

With D/H known Equation (9) was solved for L/H. Equation (9) was computer programmed and a table of values constructed. The computer program, along with samples from the table is presented in Appendix B. It should be noted that finite Q values of 1, 3, 5, and 1000 are presented in this Appendix. A quality factor of 1000 was chosen as a high Q condition. The values of Appendix B for high Q agree with those of Shaw, et al., (Ref 21:2346). The process of determining L/H then became a table look-up procedure. Because L/H is a material constant and D changes with the applied field, Equation (9) can be solved for a new D/H at $M/M_S = 0.5$. This was done by the same program as for L/H at $M/M_S = 0$. A sample of this table is also presented in Appendix B.

With a new period known for $M/M_S = 0.5$ Equation (8) was solved for a new spatial filter-bubble film distance D_{FF}.

$$D_{FF} = \underline{r}\left(\left(\frac{D}{2\lambda}\right)^2 - 1\right)^{\frac{1}{2}} \tag{15}$$

where $\underline{r}$ is the mean radius of the spatial filter and λ is the laser wavelength. Equation (15) is just the trigonom-

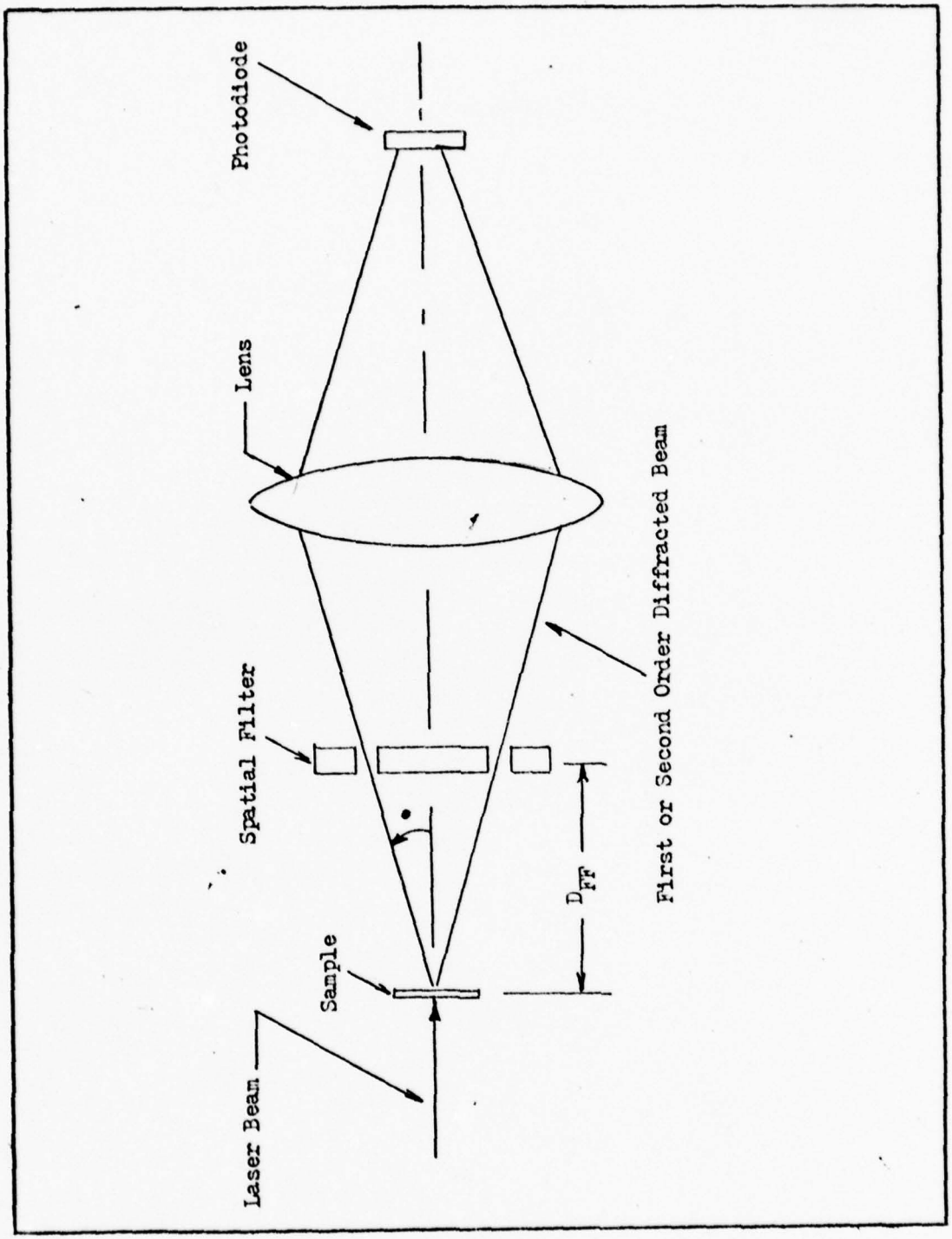

Figure 3. Basic Schematic of Diffraction Angle Measurements

etric reduction of the diffraction angle θ with n = 2. The distance D_{FF} is the distance at which the spatial filter was placed to observe the second order maximum.

Equation (10) was also programmed and a table of values computed. Appendix C lists the program and a sample from the table. The argument of Equation (10) was D/H at $M/M_S = 0.5$ obtained from Equation (9). With the spatial filter at the new D_{FF} the applied field was swept until the photodetector registered a maximum and the value of HA was measured. With HA known the value of $4\pi M_S$ was computed.

The Effect of the Quality Factor on the Measurement of L and $4\pi M_S$

One of the objectives of this study was to determine the effect of quality factor on the measurement of L and $4\pi M_S$, for 1 to 3 um films. Quality factor was studied because if static characterization is to be useful in predicting device performance the possible uncertainty in L and $4\pi M_S$ must be known. If a high Q is assumed when in fact a more modest value of Q is present ($3<Q<5$), the effect on L and $4\pi M_S$ should be known. Shaw, et al., have extensively studied this problem, (Ref 21:2346, 2349 and Ref 20:62,77) and concluded that for a D/H of 4.0 the effect on L/H is 4 percent as Q varies from 2 to infinity (Ref 20:62). It was decided to confirm this work of Shaw and investigate specifically the effect of finite Q for L/H values of .02 to .07 which are typical values for films with a stripewidth of 1 to 2 um and a thickness of 2.4 to 3.5 um (Ref 14:22). Also

investigated was the effect of Q on $4\pi M_s$ when the applied field induced a magnetization of $M/M_s = 0.5$. Quality factor was defined earlier in this thesis as

$$Q = \frac{Hk}{4\pi M_s} \tag{13}$$

following Thiele's work (Ref 22:3315). From a chart presented by Chang, the range of quality factor for Garnet films is approximately 2 to 10. The practical range presented by Chang is approximately 2 to 6 (Ref 7:171, 200).

When the Kooy and Enz equations were computer programmed the effect of finite anisotropy was considered. Finite Q values of 1, 3, 5, 1000 were chosen as representative values of low, medium and high Q respectively. These values of Q were used to plot L/H vs D/H at both $M/M_s = 0.0$ and $M/M_s = 0.5$.

Table I presents the calculated percentage change in L/H for various values of D/H as Q is changed from some low value (Q = 1, 3, 5) to an effectively infinite value (Q = 1000). This table shows that for a typical 4 to 6 um film with a D/H of 2.0 and a Q of 3 there will be a 1 percent uncertainty in the measurement of L/H. Figure 5 shows this clearly and also confirms that for D/H values of 1.50 to 2.50 and for Q>3 there is little reason to use the Q correction in the Kooy and Enz equation, unless one needs an accuracy better than 1 percent in the calculation of L/H. This plot also confirms that the industrial practice of using

a high Q value is a valid assumption for these values of D/H. However, Table I shows that as Q decreases to 1 and D/H decreases to 0.7 then the error in calculation of L/H based on the assumption of infinite Q, increases to a value of 17 percent for actual values of Q = 1 and D/H = 0.7. In present 1 to 3 um films a D/H of 0.7 is not unrealistic, although this also means that the thickness will not be equal to 4L (Ref 14:22). Figure 4 shows the spread in L/H values as D/H decreases from 1.50 to 0.50. In Figures 4 and 5 it should be noted that the error in calculation, i.e., the discrepancy in L/H values obtained, is largest for true values of Q ranging from 1 to 3 and drops considerably for values greater than 3. Fortunately, most bubble films possess Q's of approximately 3.

Figures 6 and 7 show results similar to Figures 4 and 5 for D/H values of 0.50 to 2.50 at $M/M_s = 0.5$. It can be seen that the uncertainty of L/H is approximately the same at the 1/2 magnetization point as at zero magnetization. This means that if the Henry procedure is to be used to find $4\pi M_s$ from D/H using L/H as material constant, a maximum of 34 percent uncertainty could be induced. For example if zero field D/H is 0.7 and Q = 3 then the uncertainty in L/H is 7 percent. If this value of L/H is used to find the new D/H at 1/2 magnetization, another 7 percent uncertainty in L/H is added for a total of 14 percent.

Table II shows that if D/H is 0.9 at 1/2 magnetization and Q = 3, only a 1.0 percent difference in $4\pi M_s$ for Q = 3

and Q = 1000 will be observed. A D/H of 0.9 at 1/2 magnetization corresponds to a high Q film with a zero field D/H of 0.7. Figure 8 shows the total uncertainty in $HA/4\pi M_s$ as a function of L/H, with L/H as a material constant. This figure shows the total uncertainty in using the industrial approach to find $4\pi M_s$ using the high Q assumption when in fact more likely values of Q ($3<Q<5$) are present.

The conclusion that can be drawn from this portion of the study is that the industrial practice of assuming high Q and using this to eliminate the Q dependence in the Kooy and Enz equations will lead to approximately a 5 percent uncertainty in $4\pi M_s$ for films with a zero field D/H of 1.5 and Q = 3. For films with a zero field period of 0.7 and $Q<3$, corresponding to present 1 to 3 um film, an uncertainty of approximately 13 percent will be incurred. For Q values less than 3 the maximum uncertainty in $4\pi M_s$ could be as high as 34 percent with a zero field period/thickness of 0.7 and Q = 1.

Table I

Percent Differences for L/H, M/M_S = 0.0

D/H	Q from 1 to 1000	Q from 3 to 1000	Q from 5 to 1000
.7	+17%	+7%	+4.5%
1.5	+12%	+4%	+2
2.0	+6%	+1%	0.5%

Table II

Percent Differences for $HA/4\pi M_S$, M/M_S = 0.5

D/H (M/M_S = 0.0)	D/H (M/M_S = 0.5)	Q from 1 to 1000	Q from 3 to 1000	Q from 5 to 1000
0.7	.9	-3%	-1.0%	-1.0%
1.5	1.9	-7.5	-3%	-2%
2.0	2.6	-9%	-3%	-2%

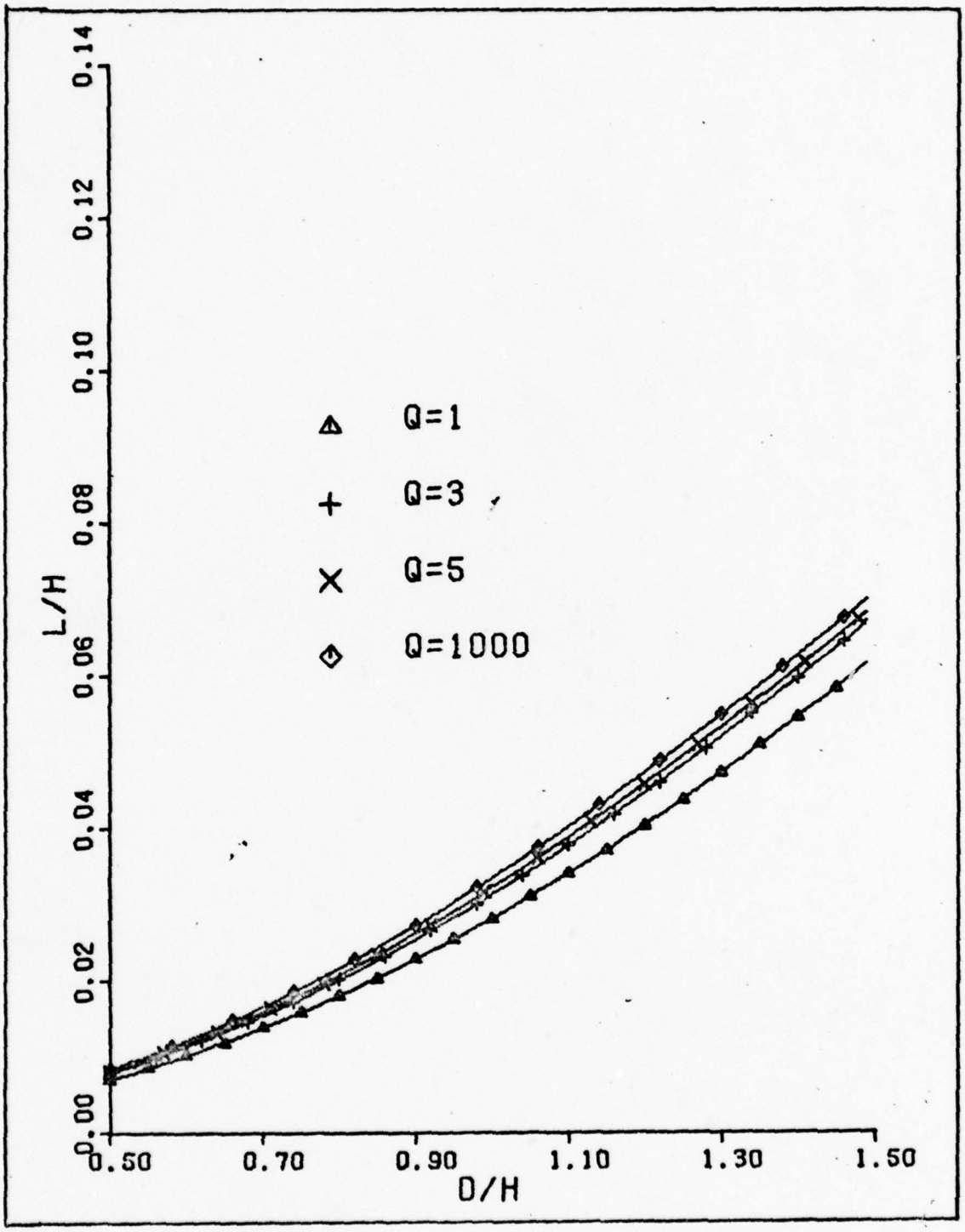

Figure 4. L/H versus D/H for various Q at $M/M_S = 0.0$, D/H from 0.5 to 1.5

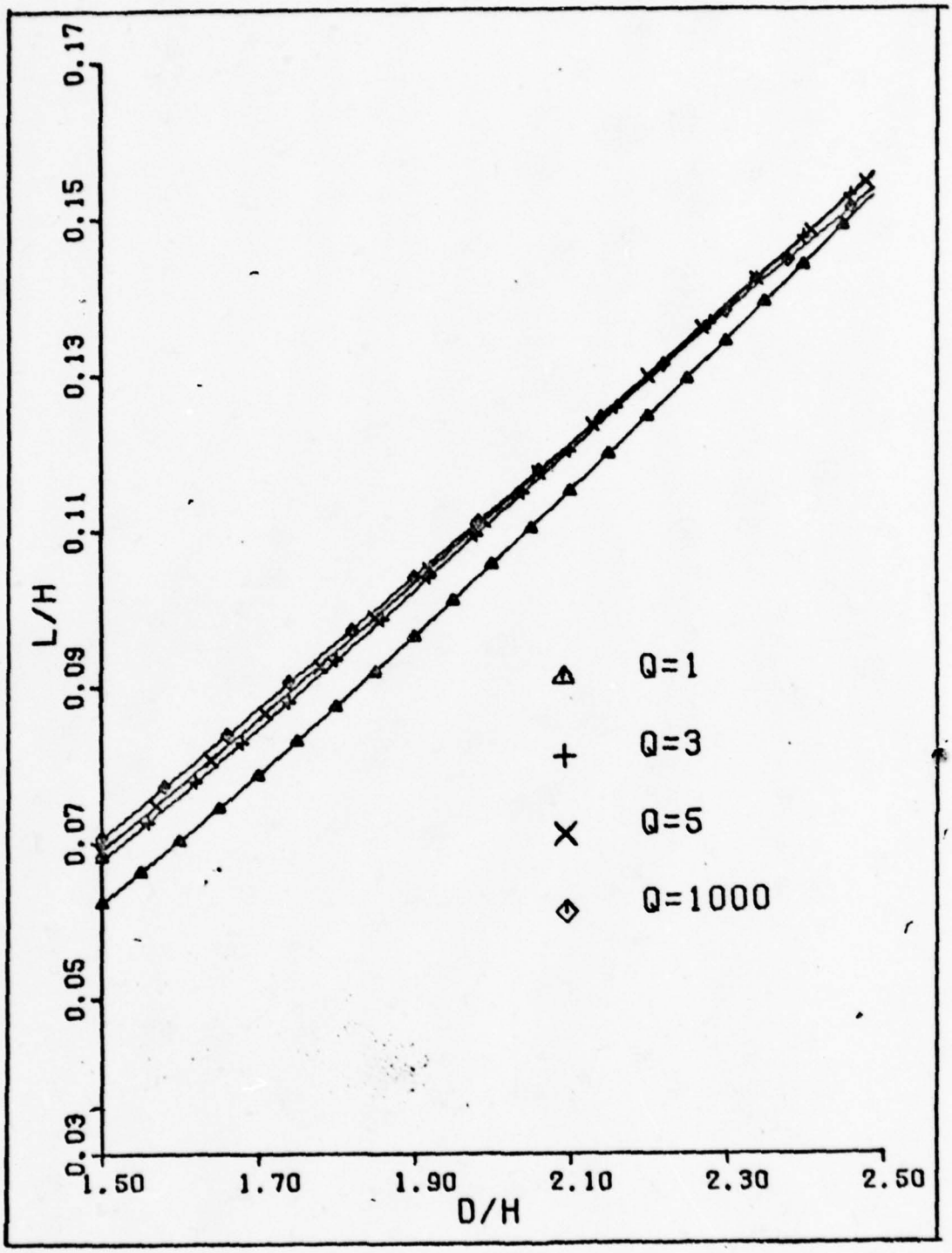

Figure 5. L/H versus D/H for various Q at M/M_S = 0.0, D/H from 1.5 to 2.5

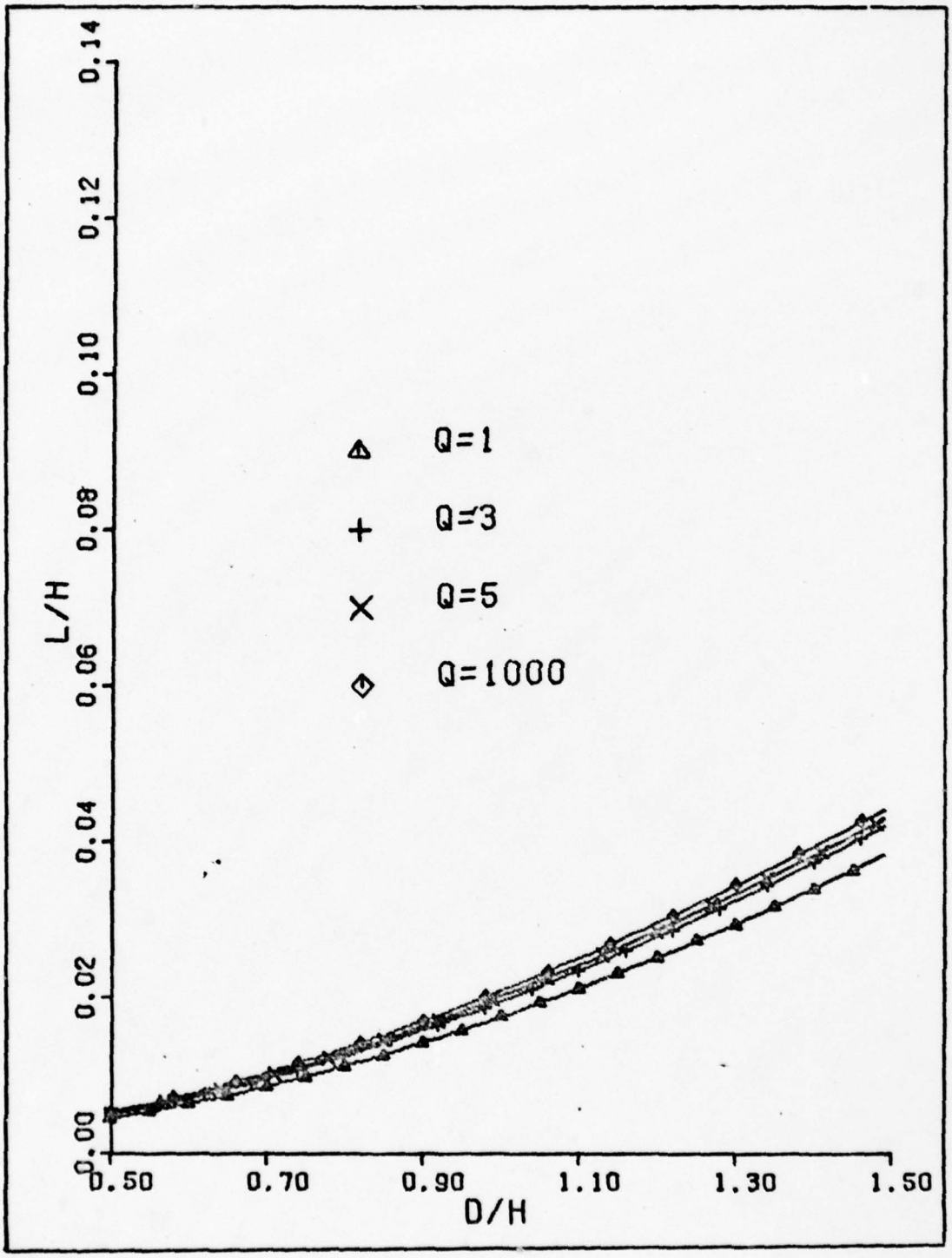

Figure 6. L/H versus D/H for various Q for D/H from 0.5 to 1.5, $M/M_s = 0.5$

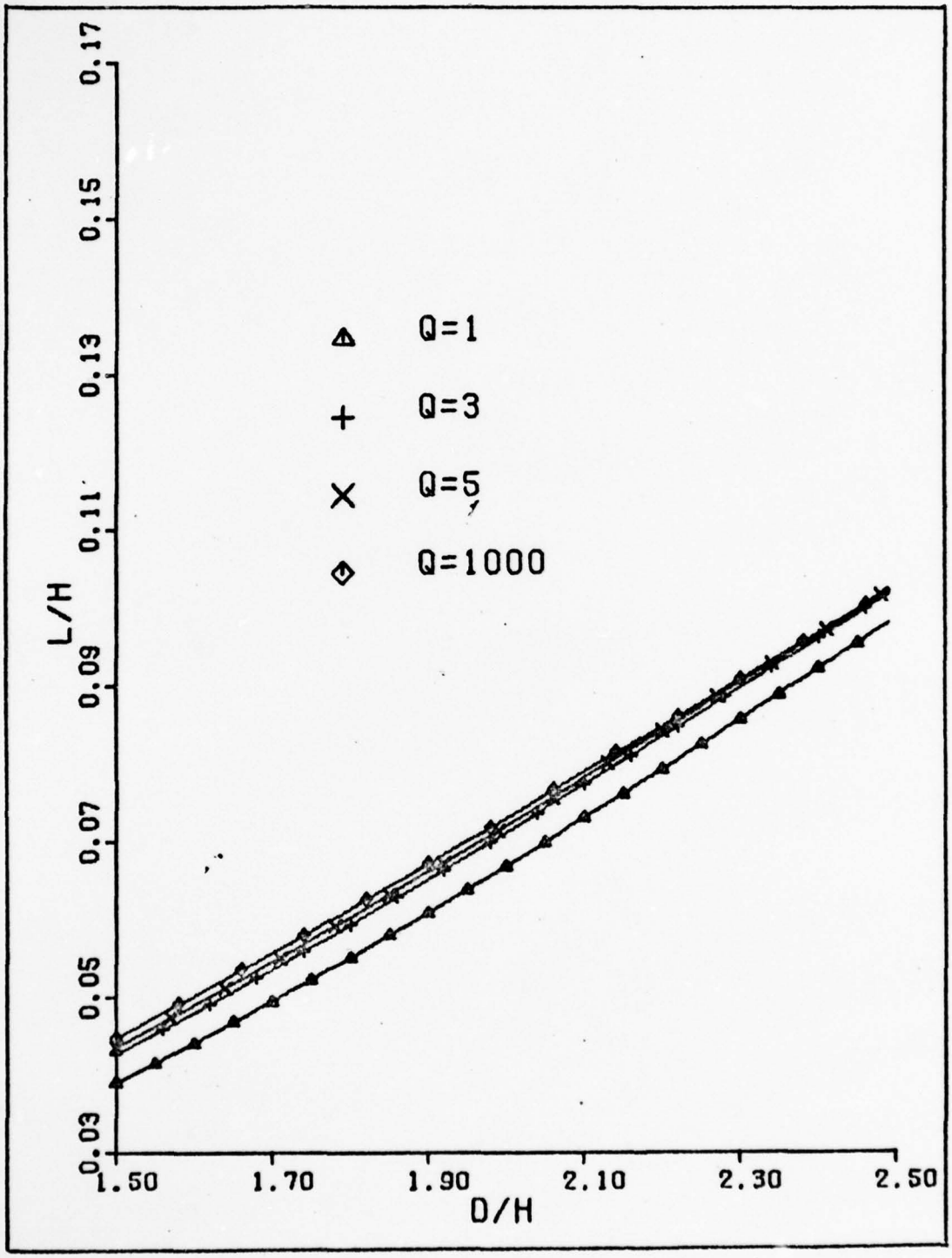

Figure 7. L/H versus D/H for various Q at $M/M_S = 0.5$ D/H from 1.5 to 2.5

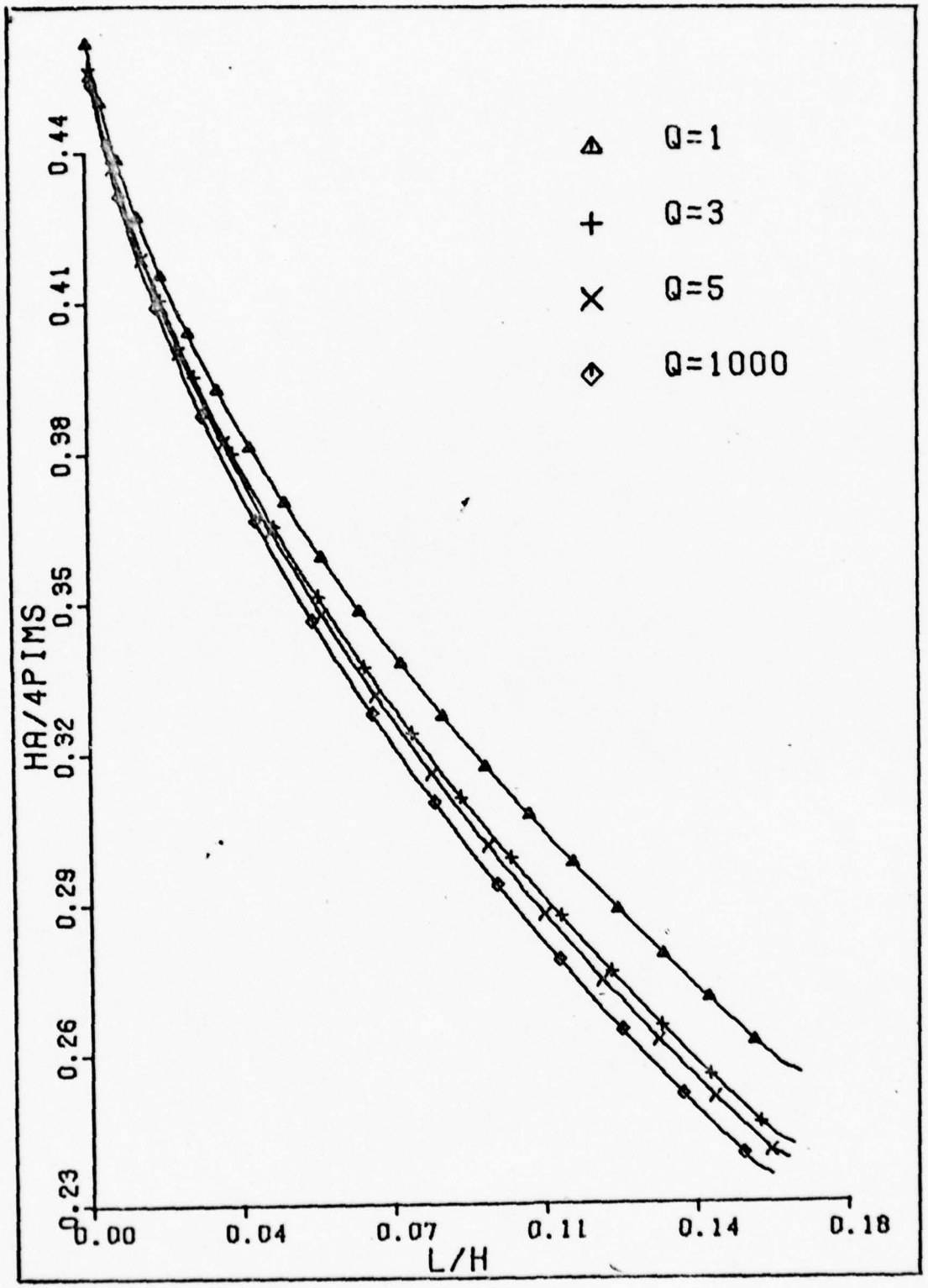

Figure 8. $HA/4\pi M_S$ versus L/H for various Q and $M/M_S = 0.5$

Sensitivity of L and $4\pi M_s$ to Small Uncertainty

This study briefly examined the question of how sensitive the Kooy and Enz equations (Equation 9 and 10) are to small variations. That is, what is the change in L and $4\pi M_s$ for a 1 percent changes in thickness, stripewidth, thickness and stripewidth together, and applied field. The computer program used was developed by Dr. M. G. Mier of AFAL, for high Q films.

The results show that if measured stripewidth is changed by +1 percent then, for a 4 to 7 um film, L and $4\pi M_s$ will change by approximately +0.1 percent. If thickness is changed by +1 percent then L and $4\pi M_s$ change by +0.5 percent. If stripewidth and thickness together change by +1 percent then L and $4\pi M_s$ change by +0.4 percent. Finally if HA changes by +1 percent L does not change and $4\pi M_s$ changes by +1 percent.

These small changes indicate that if stripewidth, thickness and applied field could be measured within 1 percent it can reasonably be concluded that the calculated parameters of L and $4\pi M_s$ will be within 1 percent. It should be noted however that these small changes are for 4 to 7 um stripewidths with an D/H of approximately 2.0. For 1 to 3 um stripewidths with D/H = 1 the results are unknown.

III. The Experimental Apparatus

Introduction

The experimental apparatus was set up in four different configurations. The first configuration used a 1.8 milliwatt (mw) HeNe laser and camera arranged as in Figure 11 (the laser is not shown but is to the right in the photograph) to take polaroid photographs of the diffraction phenomenon at zero applied field. The second setup used the same 1.8 mw laser and a spatial filter obtained from a phase contrast microscope in an attempt to measure $4\pi M_s$. It was found that this filter had a wide pass ring and required a large modulation field in the coils. The modulation field for this second setup was approximately 25 oerstads (Oe) and was obtained by the use of a Kepco Bipolar Op-Amp power supply that could also be DC biased to provide a constant DC field, HA. It was found that the 1.8 mw laser did not provide enough diffracted light to be detected by any means available when 1 to 3 um stripewidth films were tried, so a 15 mw, HeNe laser was substituted and used for all subsequent testing. The third arrangement used the 15 mw laser and coil structure shown in Figure 12. It became apparent that the Kepco power supply could not provide enough DC bias to saturate the samples for repeatability studies and "tickler" coils were mounted inside the large coils (see Figure 10) to provide the modulation field while the 5 in

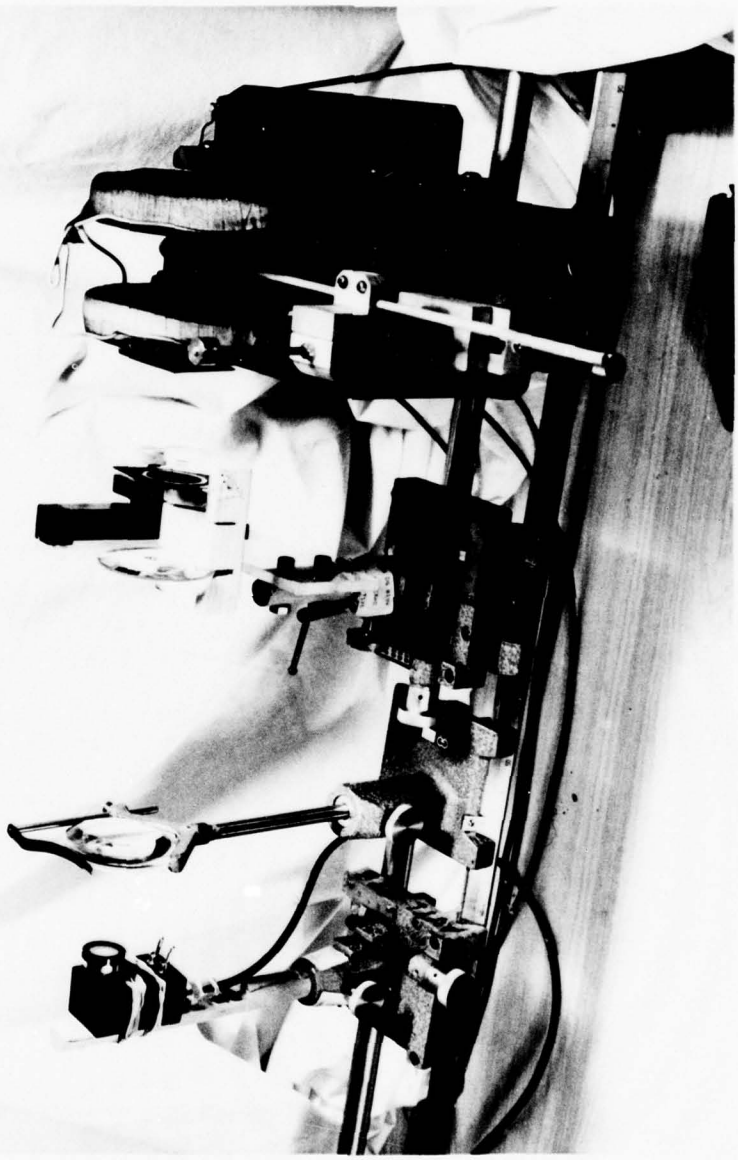

Figure 9. The Experimental Setup for Measuring W and $4\pi M_s$ Using type 505 Photodetector

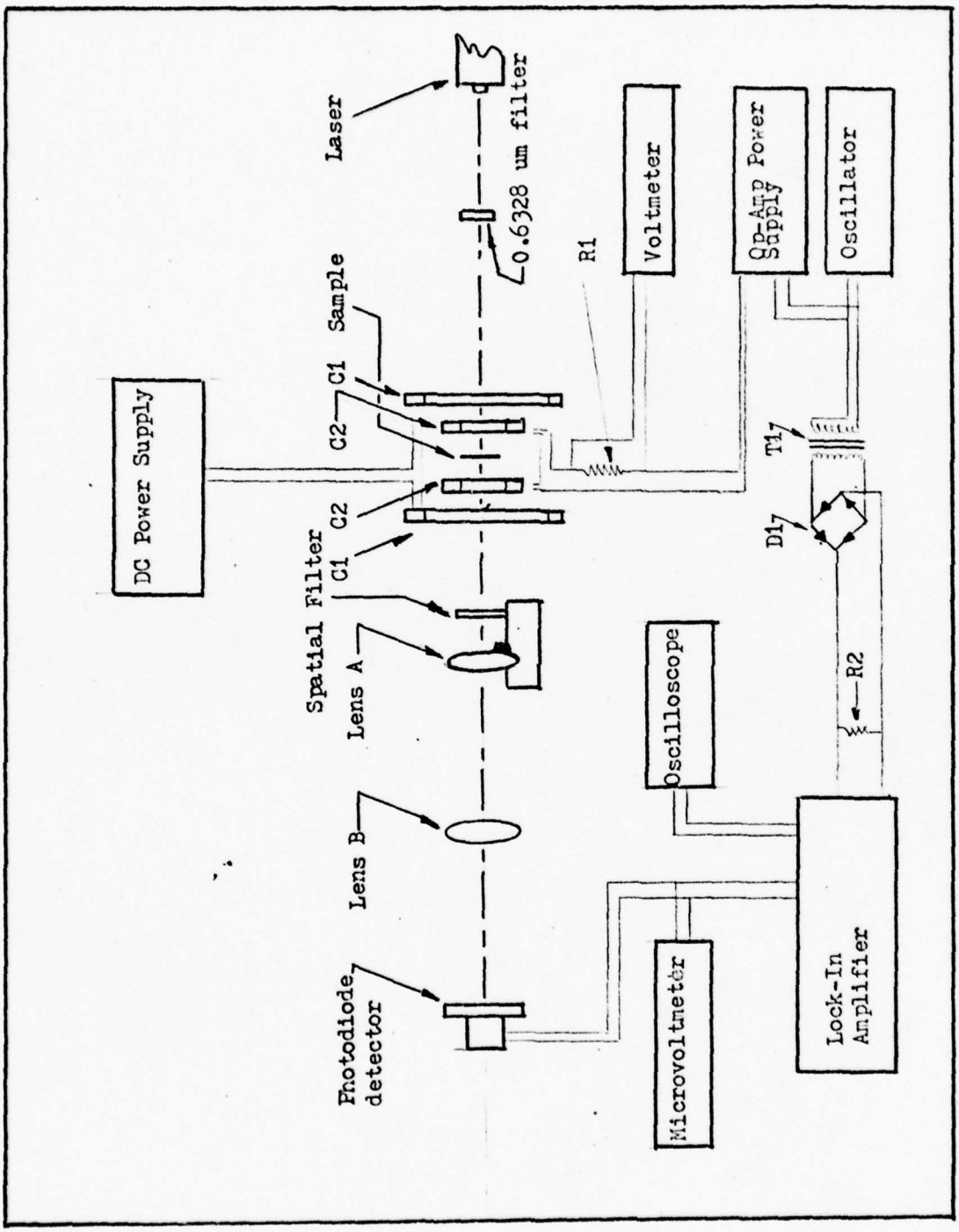

Figure 10. Schematic Diagram of the Experimental Setup. See Appendix A for Equipment Description.

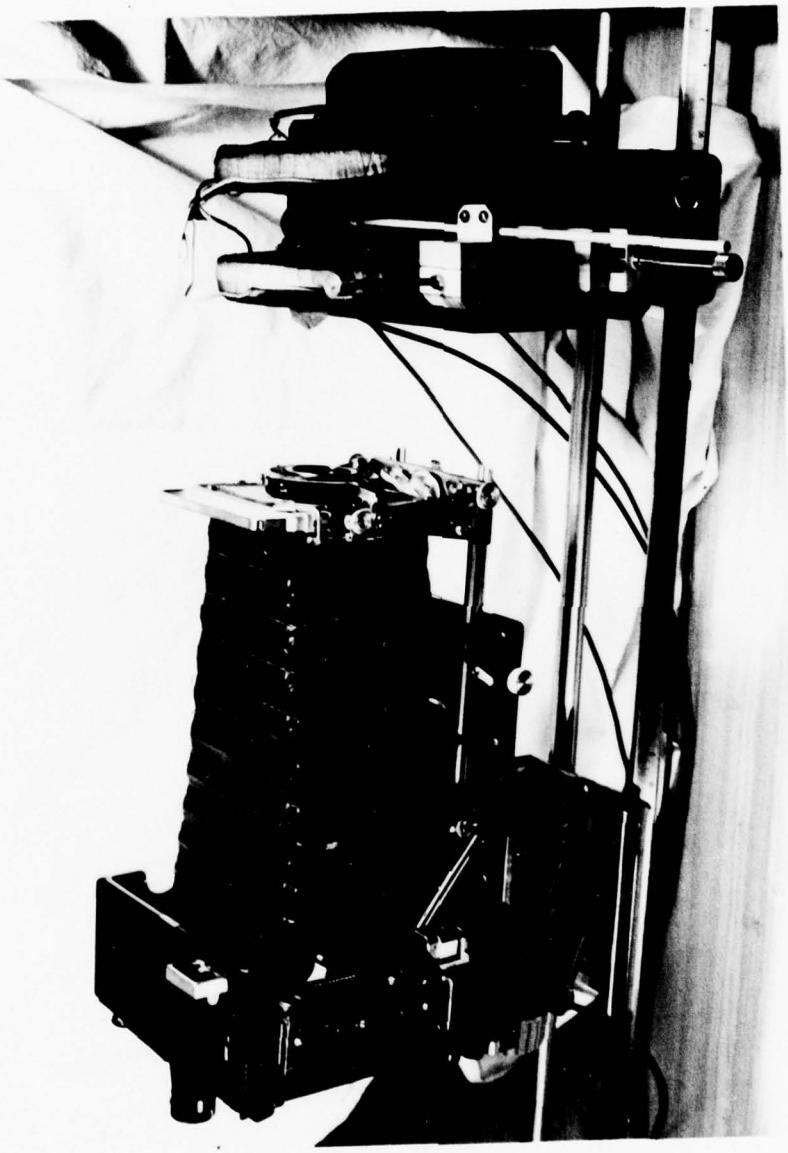

Figure 11. The Experimental Setup for Taking Pictures of Basic Diffraction Phenomena

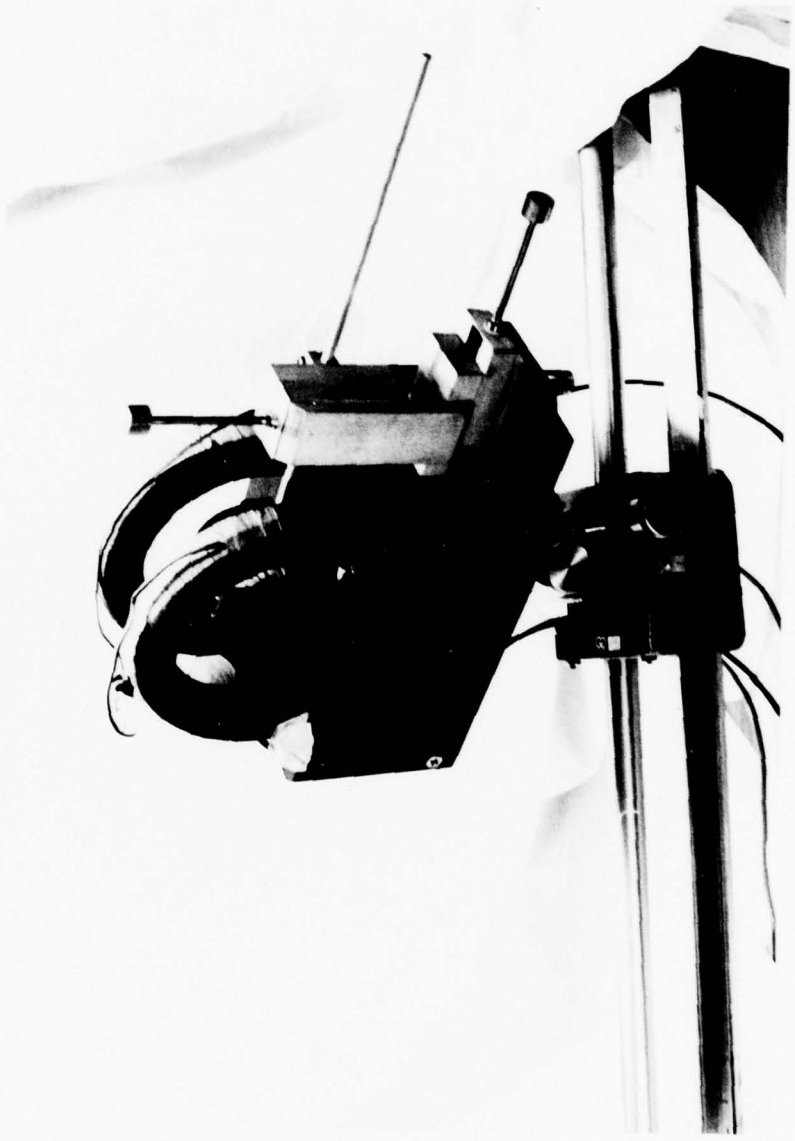

Figure 12. Photograph of the Coil and Sample Holder

coils were powered by a 60 volt, 9 amp DC power supply. The 5 in coils were then used only for HA. The fourth setup used the coil structure, 15 mw laser and camera for more diffraction studies in an attempt to discover the cause of the difference between published and experimental values in W and $4\pi M_s$. All equipment was mounted on a Gaertner optical bench with Gaertner nodal mounts. A lens was used to focus the spatially-filtered diffracted signal onto the surface of a photodetector. The output of the photodetector was amplified and fed either to a DC microvoltmeter or, if AC modulation of the "tickler" coils was used, to a derivative detection system employing a Lock-In amplifier. The position of the filter could be more accurately determined using derivative detection. Derivative detection was also employed in the measurement of $4\pi M_s$.

Light Source

The initial light source was a 1.8 mw Spectra physics model 133 HeNe laser operating at 0.6328 um. This laser was used for initial diffraction studies and for initial attempts to obtain W and $4\pi M_s$, however, when 1 to 3 um material was tried it was found that there was not enough diffracted light in the first order for zero field calculation of W. A Spectra Physics, Model 124-B, 15 mw HeNe laser operating at 0.6328 um was substituted. The 15 mw laser provided enough first order diffracted light for all samples and improved the signal-to-noise ratio in 4 to 7 um material by a factor of 10. This laser was used for all subsequent

work.

The 1.8 mw laser was spaced approximately 10 cm from the bubble film and no plasma tube light was observed. The 15 mw laser was found to emit a blue plasma tube light that was effectively polarized and would thus diffract, giving false readings. Two peaks were found of almost equal intensity for first order diffraction, separated by approximately 4 cm for nominal 4 um film (Sample 3-18-16). This problem was solved by the addition of an Oriel Co. 0.6328 um filter with 75 percent transmission effectiveness. Additionally, the laser was moved to approximately 60 cm from the bubble film to reduce intensity variations. The intensity variations from the laser, when the laser was at 10 cm, were sufficient to cause scattered reflections and reduce the diffracted signal intensity. The 15 mw laser instruction manual shows that at 60 cm from the exit pupil most of the intensity variations have attenuated or dispersed sufficiently for the beam power versus area curve to follow a smooth distribution (Ref 18:7). By moving the laser to a point 60 cm away and installing the 0.6328 um filter between the output pupil and the bubble film, the signal-to-noise ratio was improved and the width of the diffracted ring reduced from approximately 3 cm to 2 cm for a nominal 5 um stripewidth sample (TI 5696).

The final form of the measurement used to characterize the selected films consisted, then, of a 15 mw HeNe laser operating at 0.6328 um located approximately 60 cm from the

bubble film. The exact distance was not critical and depended on the variable location of the bubble film. A 0.6328 um transmission filter was placed 30 cm from the laser exit pupil and optically aligned by micrometer screw adjustments located on the filter mount. This arrangement was used in the W and $4\pi M_s$ studies of 4 to 6 um and 1 to 3 um films, and is shown schematically in Figure 10.

Photographing Diffraction Patterns

Diffraction pattern polaroid photographs were made in the initial setup of the study and near the end of the study (Figure 11). The photographs are all similar to Figure 19 and were made by placing a Graflex camera on a laboratory jack and mounting the lab-jack on the optical bench. The diffraction pattern was focused on a ground glass screen and aligned with the camers back; then a polaroid picture back was mounted and the film exposed.

Measurements of diffraction angle were attempted by measuring the magnetic film to photographic film distance and the mean pattern radius. The mean radius was calculated by dividing the pattern into segments, measuring an inner diameter and outer diameter for each, and then finding the mean radius.

Statistical calculation of the standard deviation for these eight measurements show that no more than three figure precision can be obtained for the mean radius, limiting the resultant stripewidth value to three significant figures. For example, the data in Table III were obtained from sample

3-18-16 on 20 June 1977.

Table III
Measurements of Diffraction Pattern Diameters

Sample 3-18-16	Date 20 June 77
Inside Diameter	Outside Diameter
1.852	2.268
1.813	2.236
1.835	2.306
1.830	2.318
1.841	2.317
1.848	2.344
1.880	2.332
1.828	2.326

The average inside diameter is 1.84 in with a standard deviation (sd) of 0.02. The average outside diameter is 2.32 in with a sd of 0.03.

The formula (Ref 6:43)

$$r = \bar{r} \pm \frac{sd}{(n-1)^{\frac{1}{2}}} \tag{16}$$

where n is the number of trials yields an average radius of

$$r = 1.04 \pm .05 \text{ in} \tag{17}$$

The distance from the bubble film to the polaroid plate was measured at 13.564 in with a sd of .003 in. This value is much more accurate than the radius measurement, and there-

fore the sd was neglected. When the radius measurement and film-polaroid film distance are converted to a diffraction angle, and this diffraction angle used to calculate zero field stripewidth, a value of 4.14 (1± .08) um is obtained. This compares to within 1 percent of the value obtained by other methods.

This type calculation was made at the start of the study and sample calculations such as the one above showed that information regarding the stripewidth was available in the diffraction pattern. Problems with repeatability and differences between published and experimental values did not appear until later in the experiment.

Signal Detection

The signal detection scheme, arrived at experimentally, consisted of a 10 cm focal length lens (Lens A, Figure 10) co-mounted with the spatial filter. This lens focused the spatially-filtered, diffracted beam onto the surface of the photodiode detector. Another lens (Lens B, Figure 10) with a 5 cm focal length was used with 1 to 3 um stripewidth material to shorten the focal distance required by the larger diffraction angle.

Initially a RCA 1P28 phototube with a S-5 spectral response was used in conjunction with a 500-1000 volt variable voltage DC power supply. The photo tube that Henry used, with a S-4 response was unavailable (Ref 10:1289). The S-5 tube response has a peak wave length of 3400 ± 500 Angstroms and was found to be totally unsuitable for two reasons.

First, the response at 0.6328 u is less than 10 percent of that at the peak wave length (RCA tube manual) and second, the elimination of ground loops to the Lock-In amplifier proved impossible. Sufficient 60 cycle AC noise was present in a path from the phototube to the power supply and from the phototube to the phase lock amplifier to obscure the signal below a modulation field of 25 Oe.

A United Detector Technology, Model UT505, PIN silicon photodiode and low noise transresistance op-amp mounted together in a single package was substituted. The UT505 operates on internal Mercury cells thus eliminating the ground loop problem of the phototube. The UT505 has two levels of internal amplification and the "High" level proved to be the most satisfactory. The exact amplification of the "High" level is unknown because the value of the feedback resistance in the FET op-amp is not known, however, the "High" sensitivity level is used, according to the manufacturer's data, for light levels from 10^{-12} watts/cm^2 to 10^{-7} watts/cm^2. The UT505 has an essentially flat response from 0.6 um to 0.9 um wave length and provided a typical signal level of 1.5 uv DC for a nominal 5 um film (TI 5696).

After the polarized laser beam passes through the sample and is diffracted all the Ix orders reach the spatial filter. The y-orders are removed by the polarizer, P1, in Figure 10. The calculation of W the first order beam, Ix1, is selected by the spatial filter pass-ring. Lens A, comounted with the spatial filter is used to focus the beam

onto the photodetector surface. Lens A Figure 10, is a 63 mm, 10 cm focal length double convex lens, co-mounted with the spatial filter. Lens B, Figure 10, is a 5 cm focal length, double convex lens used to shorten the focus distance when 1 to 3 um films are tested, because the approximately 10^{o} diffraction angle of 1 to 3 um stripewidth films causes the focal distance to be longer than the available length of the optical bench.

The first order diffracted light collected by the lens and focused on the photodiode is a maximum when the spatial filter is positioned so the diffracted ring is centered on the pass-ring of the spatial filter. The spatial filter was then positioned to maximize the voltage output of the photodiode, and finally the photodiode was moved along the optical bench again to maximize the output voltage.

The zero DC field stripewidth measurements used two schemes to measure the maximum voltage of the photodiode. The first used a Hewlett-Packard DC microvoltmeter which simply measured the DC voltage response to the collected light of the photodiode. The second technique employed a Princeton-Applied Research Lock-In Amplifier and a small sinusoidally modulated AC field.

In initial studies the AC field was applied by a modulating voltage applied to the 5 in coils, C1, in Figure 10. The modulating voltage was supplied by a Hewlett-Packard oscillator and fed to a Kepco, Bipolar, Op-Amp power supply. The Kepco power supply had a DC voltage offset capability

used to saturate the domains between tests for repeatability studies. It was found that the DC offset capability was not sufficient to saturate the domains, because for a nominal 5 um stripewidth material a DC applied field, HA of at least 50 Oe is required. The 50 Oe figure for saturation was obtained from Bobeck, who shows magnetization curves for various values of crystal thickness. Saturation is defined as $M/M_s = 1.0$, and for a typical H = 4L, $HA/M_s = 0.25$ (Ref 3: 26). Then for an M_s of 200 G (typical value for nominal 5 um films) HA must be 50 Oe. The Kepco Op-Amp with an AC field of less than 10 Oe would only supply a DC field of 40 Oe. Separate modulation coils were then installed, C2, in Figure 10, and the AC field was supplied by the Kepco power supply. The Kepco power supply was sinusoidally modulated by a Hewlett-Packard oscillator.

The basic assumption in applying the modulation field was that the AC field would move the domain walls slightly thus varying the diffraction angle as the stripewidth varied, without changing the average W. This varying diffraction angle would cause a sinusoidal signal to be detected by the photodetector at twice the frequency of the modulated field when the filter was at location B in Figure 13.

It can be seen from Figure 13 that when the spatial filter was at position A or C the frequency of the detected signal was the same as the modulated signal. As the filter approached position B the double modulation component increased until the mean beam position was exactly centered in

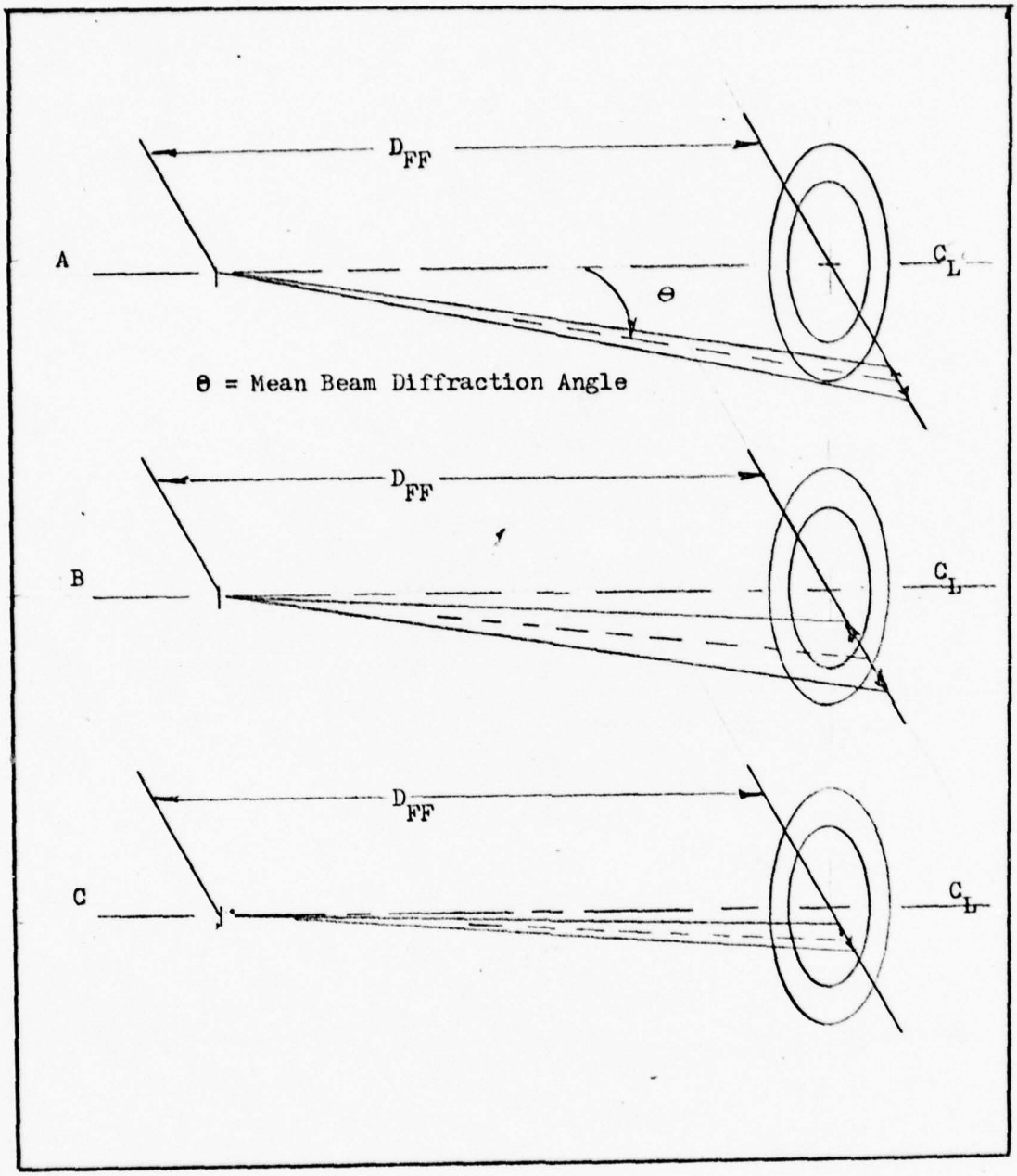

Figure 13. Location of 2X coil modulation Signal. A shows diffracted signal outside of pass ring. B shows the signal centered, causing a 2X signal to be detected. C shows the diffracted signal inside the pass ring.

the pass-ring of the spatial filter.

A reference signal was obtained from the oscillator driving the Kepco power supply. The reference signal was fed to a full-wave bridge rectifier used as a frequency doubler. A 12V filament transformer was used as isolation between the oscillator and the bridge rectifier to prevent loading of the power supply by the bridge. A 100 K-ohm resistor was found to be needed to match the input impedance of the Lock-In amplifier.

The doubled rectified reference frequency was fed to a Princeton-Applied Research Lock-In amplifier, Model HR-8, with a Type C preamplifier. The Lock-In amplifier is essentially a detection system with an extremely narrow equivalent noise bandwidth. The basic element is a phase-sensitive detector in which the signal voltage is mixed with a reference voltage, producing sum and difference frequencies. A low-pass filter at the output of the mixer rejects the high frequency components that constitute sum frequencies and passes the difference frequencies that lie within the low-pass filter passband. The difference frequency when the signal frequency is exactly the same as the reference signal is zero. The phase difference between the signal and reference is adjustable on the Lock-In amplifier and was monitored by the oscilloscope indicated in Figure 10. The output of the low-pass filter was due to the portion of the signal spectrum lying about the reference frequency within the pass band of the low-pass filter (Ref 13:1/1). As the

doubled modulation component of the signal increased the output of the mixer decreased until point B, Figure 13, was found. Point B, Figure 13, constituted a null in the Lock-In amplifier and was indicated as a null on the voltmeter output of the Lock-In amplifier. This null detection system constituted derivative detection of the doubled modulation frequency using the output of the low-pass filter/mixer stage of a Lock-In amplifier as a null detector. This enabled the mean diffraction angle to be obtained much more precisely than with the microvoltmeter.

It was found experimentally that the lowest value of AC field that could be detected by derivative detection during stripewidth studies was 8 Oe RMS and during $4\pi M_s$ measurements, 3 Oe RMS. The lowest usable scale on the Lock-In amplifier was the 5 uv scale; below that range electrical noise, of undetermined origin, obscured the signal and the amplifier could not lock onto the signal.

A fundamental coil modulation frequency of 100 Hz was selected experimentally as the best frequency for testing. This range allowed a circuit Q of approximately 15 with a rise time of 300 msec to be selected on the Lock-In amplifier. Higher frequencies were tried but the AC field was limited to 400 Hz by the capabilities of the Bell, Model 615, Gaussmeter used to measure the field. Higher frequencies, up to 1.0 KHz, increased the noise level of Lock-In amplifier and thus required a larger AC field to modulate the stripewidths. The noise level increased because of the

finite rise time of the UT 505 in the "High" amplification position.

A cardboard box was painted black and placed around the apparatus, and a black curtain was placed over the box to further remove light leaks. The room lights were also extinguished during testing, because the fluorescent lights were found to produce electrical noise in the Lock-In amplifier.

Coil Structure and Field Generation

Figure 12 shows the coil arrangement with the coil and sample holder while Figure 10 shows the electrical and placement schematic. The coils, C1 and C2 in Figure 10, were used because they were available in the Electronic Research Branch of the Air Force Avionics Lab.

The large coils were used in the final arrangement to provide a DC field, HA only. The large coils, C1, had an inside diameter of 4 in and were wound with 300 turns of #18 AWG copper wire. The small coils had an inside diameter of 1.5 in and were wound with 100 turns #20 AWG copper wire. Both sets of coils were placed in the Helmholtz condition, that is, the coils were placed a mean radius apart. The large coils, C1, were placed 1 3/8 in apart while the coils C2, were placed 1 in apart.

A Bell, Model 615, Gaussmeter with a 10X probe was used to measure the field. It was found that the field was uniform along the axis of the coils for ± 3/8 in from the center of the coils. The magnetic film sample was placed in

the approximate center of the coils, on the centerline. The coils C1 had a maximum DC field at the center point of 230 Oe at 10 A DC. The small coils, C2, had an RMS maximum AC field to 100 Hz of 100 Oe. A 2 ohm resistor, R1, was placed in one supply lead of the C2 coils and a voltmeter connected across the resistor to measure the voltage drop. The small coils were then calibrated against RMS AC voltage for convenience in establishing a known AC field for subsequent testing. For example 1.5 V RMS corresponded to an 8 Oe RMS field. The DC field was measured each time it was used (in $4\pi M_s$ measurements) directly in front of the sample, on the centerline between the laser and the sample.

The coils C1 were powered by a NJE Corp, Model CR60-9, 60-V, 9-A power supply. The AC coils were driven by a Kepco, Op-Amp power supply with the frequency source being a Hewlett-Packard, Model 200CD, oscillator.

Sample Preparation

The samples were chosen from those available in the Air Force Avionics Laboratory, Electronics Research Branch, Wright-Patterson Air Force Base, Ohio. Several cleaning methods were tried. The first method used trichloroethylene and acetone, followed by 2 to 3 minutes of ultrasonic cleaning in freon. The second method used only a wash in an Alconox laboratory glassware soap solution followed by a rinse in warm water. A cotton-tipped applicator stick was used to scrub the samples while in the Alconox solution. The second method proved adequate for subsequent optical

testing.

All samples were mounted in a slit cut in a 1/8 in wooden dowel rod. The dowel rod fitted into the adjustable sample holder that is shown in Figure 12.

One sample was etched in boiling phosphoric acid to remove the garnet layer from one side of the double-sided wafer. The sample (1-9-3) was prepared by ultrasonic rinsing in trichloroethylene, followed by acetone and then freon for 2 to 3 minutes. A section of one side of the 2 by 3 cm sample was then coated with General Electric Co. Room Temperature Vinyl and allowed to cure for 24 hours. The sample was then boiled in phosphoric acid for 30 minutes at 150°C. The vinyl was removed using a commercial solvent, Dynasolve, and the sample cleaned in an Alconox solution. It was then mounted on a dowel rod for optical testing.

Three techniques were used to magnetically prepare the sample. In the first method, the coils C1 were powered to the maximum DC field, 230 Oe, and then the DC power supply was switched off. It was assumed that the domains would return to some average stripewidth and give better repeatability and more accurate results. The second method involved gradual application of a DC field, by means of the current-limiter control on the NJE power supply, and then return of the field to zero using the same control. Finally, when Henry published his preconditioning technique, a similar method was tried. Henry used a slow (10 second period) saturating sine wave applied simultaneously with a

small (5 Oe) 20 Hz field (Ref 12:1529). This third technique applied a 100 Hz AC field to the sample and gradually increased the amplitude to a maximum of 100 Oe in coils C2. Then the field was gradually reduced to zero. If derivative detection was employed, the AC field was then reset to the desired value of 8 Oe for stripewidth measurements and 3 Oe for $4\pi M_s$ measurements.

Spatial Filter Design, Construction and Mounting

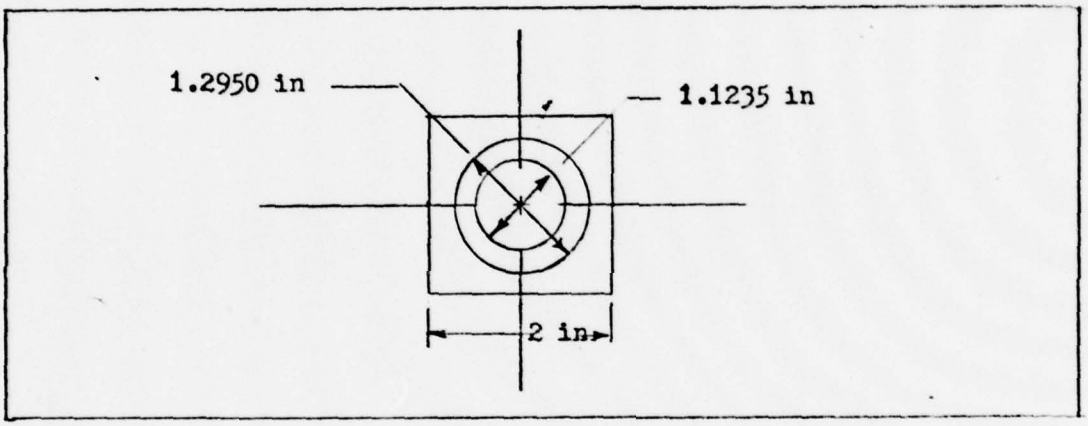

Figure 14. Geometry of the Spatial Filter, Final design

Henry utilized a metallized glass sheet with an annular pass-ring width of 1.0 mm and a mean radius of 1.0 cm (Ref 12:1528). The pass-ring width is 1/2 of the difference between the inner and outer diameters. Originally in the Electronic Research Branch installation it was desired to use a ready made filter obtained from a phase contrast microscope. This filter had a mean radius of 0.86 cm (0.34 in) and a pass-ring width of 0.13 cm (0.05 in). Three problems

became apparent with this ready-made filter: first, it could not be positioned close enough to the film to detect the second order maximum for 1 to 2 um bubble films; second, the width of the pass-ring was excessively wide making the modulated signal extremely weak; and third, the actual filter was located between two pieces of glass making an accurate determination of mean-radius and pass-ring width impossible.

Design of a new filter was initiated with the intent of having one filter suitable for both 4 to 6 um and 1 to 3 um bubble films. The minimum distance from the film in the film holder to the spatial filter was approximately 3.25 in. This minimum distance arises from interference of the coil-holder optical bench mount and the spatial-filter holder optical bench mount. For a typical 5 um thick film the zero field stripewidth is approximately 6 um (Ref 4:252). The minimum mean diameter of a filter for these films was then computed from Equation (8). The minimum diameter is 0.4 in for a film holder-filter distance of 3.25 in. For a typical 2 um thick film the zero field stripewidth is approximately 1.7 um (Ref 14:22). This corresponds to a minimum diameter of 1.3 in. A mean filter diameter of 1.3 in was thus chosen as the best value for both 4 to 7 and 1 to 3 um stripewidth films.

Two pass-ring widths were chosen: 0.030 in and 0.040 in. It was believed that one of these would provide both a sufficiently modulated signal at 2 Oe and enough transmitted

light to be detected.

An attempt was made to construct these filters in the AFIT Coop Laboratory. First two brass rings were machined out of available material, one with an inner diameter of 1.1235 in and outside diameter of 1.295 in, and another with a 1.215 in inside diameter and a 1.295 in outside diameter. While both these rings have mean diameter less than that required for 2 um thick films this was the only size material available. Glass plates, 2 in by 2 in were then cleaned in detergent, followed by trichloroethylene, acetone, and methanol rinses. The glass plates were aluminized using vacuum evaporation equipment in the Coop Laboratory. The aluminized plates were coated with photoresist and the machined ring placed on top. The photoresist was then exposed to 15 seconds to a mercury light. The ring was then removed and the photoresist developed using xylene and butyl acetate. The aluminum was then etched for approximately 1 min in a mixture of phosphoric acid (120 ml), nitric acid (7 ml), glacial acetic acid (7 ml), and de-ionized water (130 ml). This left an aluminum-plated glass slide with an appropriate pass-ring.

Unfortunately several events combined to produce only one usable filter. One slide was improperly cleaned and the aluminum peeled off during the photoresist process. One slide was not exposed properly, and consequently the ring did not develop. Another slide was over-etched during the etching process, resulting in an unusable filter.

The one usable filter obtained from the Coop Laboratory has an inside diameter of 1.235 in an outer diameter of 1.295 in. This filter was utilized in the present study and has a mean radius of 0.6325 in.

It was found experimentally that alignment of the spatial filter was critical. The spatial filter was then mounted on a block of wood with Lens A, Figures 9 and 10. Finally the block of wood was mounted on a surplus microscope x-y stage which provided horizontal and vertical adjustment of the filter. The signal could then be maximinized by the x-y adjustments of the stage.

Measurements and Accuracy

The basic measurement of length required was the sample-spatial filter distance, D_{FF}, Figure 10. This length was established by calibrating the optical bench to a known distance. A 9.991 in long metal rod was cut and set on a laboratory-jack, while the index on the spatial filter mount was set at a convenient centimeter mark on the optical bench. The lab jack was positioned on the optical bench, with the rod aligned parallel to the centerline; then the test sample and coil holder mount were carefully moved up until the rod just touched the center of the spatial filter and also just touched the test sample. The optical bench was then calibrated to a known position.

The optical bench had a centimeter scale with millimeter markings engraved upon it. One of the desirable objectives for the spatial filter was to increase the preci-

sion in the measurement of W from 2 significant figures to 3 significant figures. For example, if a 5.00 um stripewidth was to be measured, then D_{FF} had to be known to a precision of ±0.01 in which corresponds to ±0.25 mm. To achieve three significant figure accuracy, it was necessary to estimate the division of 1 mm by the spatial filter mount index to within 0.25 mm. D_{FF} was also needed, to the same precision, for placing the spatial filter a known distance from the sample for the measurement of $4\pi M_s$. Three significant figures were the standard of precision chosen, limited by the measurement of D_{FF}.

The Measurement of the Anisotropy Field, Hk

By positioning the coils C2 normal to the laser beam an attempt was made to generate sufficient in-plane field to detect the minimum of the Faraday rotation that should occur as the magnetization vector is pulled in-plane (Ref 20:111-114). If the field Hk was known, the quality factor could be computed, as least on a "first-try" approximation, by dividing Hk by the $4\pi M_s$ value for infinite Q.

Unfortunately the combined field of 300 Oe DC from coils C1 and C2 was not sufficient to measure even low values of Q, (for example, Q = 2) since for a $4\pi M_s$ of 200 G this required an Hk field of 400 Oe. The coils became too hot for fields larger than 300 G and further attempts to measure Hk were abandoned.

IV. Experimental Procedure

Introduction

The measurements were taken by the methods described in the Apparatus section. The following description shows how the values of W and $4\pi M_s$ (as presented in the Results section of this study) were obtained. The Fortran computer program to obtain the tables for the sample calculation is listed in the appropriate Appendix along with sample values from the tables.

Procedure Steps

1. The sample was mounted in the sample holder and positioned in the center of the coils.
2. The optical alignment of the system was checked before each sample was measured. This was accomplished by aligning each element including the sample so that the laser beam was reflected back to the laser output pupil.
3. If the Lock-In Amplifier was to be used, a known AC field was established in coils C2 using the Gaussmeter.
4. The sample was saturated magnetically with a preconditioning technique. The techniques used are presented in Figure 15.
5. The reference graduation on the optical bench was established by placing the known length measuring rod on the Lab-Jack. The index on the spatial filter mount was aligned

with a suitable mark and the sample holder brought to a known distance away. This procedure allowed the bubble film-to-spatial filter distance to be read off the optical bench scale.

6. The apparatus to be used was connected. If the microvoltmeter was to be used to record the position of the maximum intensity of diffracted light passing through the filter, no AC field was used. If the Lock-In amplifier was to be used, the output of the photodetector was connected to the input of the Lock-In and the Lock-In was tuned to twice the oscillator frequency. The reference signal of the Lock-In was checked using an oscilloscope to insure that it was the proper frequency (200 Hz). The mixer output of the Lock-In was used as a Null output for derivative detection.

7. The spatial filter was positioned either for maximum signal strength on the microvoltmeter or a null on the Lock-In.

8. The photodetection apparatus was positioned for maximum received signal and the position of the spatial filter rechecked.

9. The scale on the optical bench was read and the result converted to a value for D_{FF} in inches.

10. Using the formula

$$2 W \sin \theta = \lambda \tag{8}$$

W was calculated based on the trigonometric relationship

$$\theta = \text{TAN}^{-1}\left(\frac{.6326}{D_{FF}}\right) \tag{18}$$

where .6326 is the mean radius of the spatial filter. W was recorded.

11. Using the thickness of the film as provided by the manufacturer, D/H was calculated from the expression

$$D = 2\ W\ (\text{Zero field}) \tag{19}$$

12. Using the calculated D/H, a Table based on the results of the computer program (Appendix B) for D/H versus L/H, $M/M_S = 0.0$, was used to find L/H. The Q = 1000 column of the sample Table in Appendix B was used for all calculations. L/H is a material constant.

13. Using the same computer program of Appendix B, another table with L/H ($M/M_S = 0.0$) at the new value of M/M_S, that is, $M/M_S = 0.5$, was used to find D/H for $M/M_S = 0.5$. This table of D/H versus L/H was generated from the same program except M/M_S was changed to 0.5.

14. The new D_{FF} for the spatial filter was found from the relationship

$$D_{FF} = .6326 \left(\left(\frac{\frac{D}{H} \cdot H}{2\lambda} \right)^2 - 1 \right)^{\frac{1}{2}} \tag{20}$$

which is obtained from Equations (8) and (19) combined with n=2.

15. The spatial filter was positioned at this new D_{FF}, using the calibrated scale of the optical bench, and the Lock-In amplifier checked for setup. The AC field in coils C2 was checked to verify a known value.

16. The DC field was gradually increased until a null was detected on the Lock-In mixer output.

17. The DC field value was measured using the Bell Gaussmeter.

18. The Fortran computer program of Appendix C was used to generate a table of values for $HA/4\pi M_s$ at $M/M_s = 0.5$, using D/H ($M/M_s = 0.5$) as an argument, and with D/H ($M/M_s = 0.5$) known, a value of $HA/4\pi M_s$ was located for Q = 1000.

19. $4\pi M_s$ was calculated from

$$4\pi M_s = \frac{HA}{\text{Table value (Appendix C)}} \qquad (21)$$

Sample Calculations

Date: 26 September 1977

Sample: 3-18-18

Note: Numbers in parenthesis refer to appropriate steps under the procedure steps just listed.

(4) Saturate the sample magnetically. A manually ramped DC field was used.

(5) Set the index on the Spatial filter mount to the 57.00 cm mark on the optical bench. Set the 9.991 in measuring rod on the Lab-Jack and position one end of the rod against the spatial filter. Bring the bubble film up to the other end of the rod. This establishes the spatial filter bubble film distance as 9.991 in with a reference mark of 57.00 cm on the optical bench.

(6) Using the microvoltmeter four measurements were made of the peak output. The following reference marks were recorded for these trials:

60.62 cm
60.71 cm
60.78 cm
60.51 cm

The average is 60.66 cm which makes D_{FF} equal to 8.55 in.

(10) W is 4.29 um, from Equation (8).

(11) D/H is 2.09 where H is 4.10 um as provided by the manufacturer.

(12) Find L/H from Appendix B, for Q = 1000, M/M_S = 0.0 L/H is equal to 0.12025.

(13) Find D/H for M/M_S = 0.5 from the sample table in Appendix B. D/H is now equal 2.79.

(14) Find the new spatial filter distance. D_{FF} = 5.683 in from Equation (20), with D/H = 2.79 and H = 4.10 um. Since the 57.00 cm mark on the optical bench corresponds to a 9.991 in spatial filter-bubble film distance, the 67.94 cm mark on the optical bench corresponds to a D_{FF} of 5.683 in.

(17) The field was measured as 85.8 Oe.

(19) From Appendix C, $HA/4\pi M_S$ is 0.270791 for Q = 1000, and D/H is equal to 2.79, and M/M_S = 0.5. $4\pi M_S$ is then 316 Gauss.

These values of W, L/H, and $4\pi M_S$ are recorded in Table IV of the results section.

V. Experimental Results

Introduction

The results of the study was presented in Tables IV to XV. The results were obtained using the apparatus described in the Apparatus section of this study and using the experimental procedure of the previous section. The results show wide discrepancies in the measurement of W from expected values based on manufacturers' data. The average difference in W for 4 to 7 um films from the W of the manufacturer is 15 percent, while the average difference in W for 1 to 3 um films is 14 percent. The average difference in $4\pi M_s$ for all films is 23 percent. The notes for Tables IV to XIV are shown in Figures 15, 16, 17, and 18.

The basic assumption underlying all the measurements was that they should be repeatable within experimental accuracy because it was assumed that after any saturating magnetic disturbance the stripewidth would return to the same average value. This was found not to be the case. Different preconditioning techniques yielded different, non-repeatable results. If the films had a unique characteristic stripewidth, the measurements should have been repeatable and predictable after a magnetic disturbance. The results listed do not bear this out.

Results

Table IV shows the results for sample 3-18-16. This sample has a particularly high coercivity, 4.2 G, measured by Professor Clark Searle of the University of Manitoba, Canada (Ref 26). Photographs taken of this film in the Air Force Avionics Laboratory show magnetic and physical defects which may have caused problems with repeatability and accuracy because magnetic defects tend to distort the minimum domain energy condition. Table IV shows that for this sample, even with the same technique of preconditioning and using the same equipment, the results for W differ by -19% to +2% from the manufacturer's data. For the measurement of $4\pi M_s$, the Lock-In amplifier was used with the spatial filter positioned at the appropriate precomputed location.

Tables V, VI and VII show the results for films similar to 3-18-16 except that these films are not known to have high coercivity nor to be magnetically or physically defective. The $4\pi M_s$ measurements for TI 5696 showed differences of +15% and -25% from manufacturer's data (Table V). The $4\pi M_s$ measurements for sample 1-9-3 showed -51% and -42% discrepancies. Each time a measurement was made the apparatus was checked for alignment and the physical measurements checked for large errors.

Table VIII shows the results of measurements on sample 1-9-3. Sample 1-9-3 was prepared for single-sided film experiments as described in the apparatus section. The results show the same low value (average -30%) for W as those

in Table VII, the results for the same film, except double sided.

Tables IX, X, XI, XII, XIII, and XIV show the results for the 1 to 3 um tilms. These tables all show the same general pattern, that is, they exhibit similar ± average differences from expected values with no particular pattern. The $4\pi M_s$ measurement, only possible for films 6-20-12 (Table XII) and 6-20-11 (Table XIII), shows up to a 61% difference between the manufacturer's data and experimental results. The $4\pi M_s$ measurement made on these films is different in one respect from that of the other films. The AC field required for detection of a signal was very large, approximately 50 Oe in one case, in contrast to the fields of as low as 3 Oe required for 4 to 7 um films. Notes 9 to 13 of Figure 18 apply to these films.

Table XV shows the results of a comparison done between the Signal-Only Mode and the Phase Lock Mode of the Lock-In amplifier. In the Signal-Only Mode, the Lock-In amplifier was used as a wide band signal voltmeter with no signal-reference frequency mixing. The values in both columns are approximately the same and show no pattern for AC fields up to 40 Oe.

Figure 19 shows one reason why the measured value of W is usually lower than the manufacturer's W. For any AC field, it appears that the magnetization reduces the average stripe-width. The photographs of Figure 9 were taken using the diffraction pattern photography setup and show qualitatively

that even a small AC field of approximately 2 Oe changes the mean radius of the diffraction pattern. Figure 19, A shows the diffraction pattern after the saturation field (DC) is suddenly removed and Figure 19, B shows the effect of the application of a 2 Oe AC field following the conditions of photograph. It is believed that the diffraction radius does not change significantly between AC fields of 2 to 8 Oe. Unfortunately, the lowest value of AC field that could be detected using the Lock-In amplifier was 8 Oe which is the starting value in Table XV.

Table IV
Sample 3-18-16

Date	Data Source	Magnetic Preparation	W(um)	L/H	$4\pi M_S$(G)
----	Manuf.[1]	Unknown	4.14	.11	276
9/27	Microscope[2]	Last State	4.7 (+14%)[1]		---[2]
----	Microscope[3]	Unknown	4.07 (-2%)		---
6/17	Diffraction[6]	Last State	4.14 (0%)		
6/17	Diffraction	Last State	4.12 (-0.5%)		
9/26	Lock-In[4]	SS-SO(DC)[3]	4.21 (+2%)[3]	.12 (+9%)	287 (+4%)[3]
9/26	Microvolt-M[5] & Lock-In	SS-0(DC)	4.29 (+4%)	.12 (+9%)	317 (+15%)[3]
9/7	Lock-In	SS-0(DC)[4]	4.15 (+0.2%)[4]	.11	318 (+15%)[4]
9/7	Lock-In	SS-0(DC)	3.94 (-5%)[4]		
8/29	Lock-In	SS-0(DC)	4.09 (-1%)[4]		
8/29	Lock-In	SS-0(DC)	4.02 (-3%)[4]	.11	222 (-20%)[4]
8/19	Lock-In	Magnet[5]	4.12 (-0.5%)[4]		
8/25	Lock-In	Magnet[4]	3.98 (-4%)[5]		

Table V
Sample TI 5696

Date	Data Source	Magnetic Preparation	W(um)	L/H	$4\pi M_s$(G)
	Manuf.[1]	Unknown	4.65	.08	194
	Microscope[3]	Unknown	3.93 (-15%)[1]		
6/6	Diffraction[6]	Last State[2]	4.30 (-8%)		
6/21	Diffraction	Last State[2]	5.09 (+9%)		
9/20	Lock-In[4]	SS-O(DC)[4]	4.96 (+7%)[6]	.09 (+13%)	
9/23	Microfolt meter[7]	SS-O(DC)	5.25 (+13%)	.10 (+25%)	224 (+15%)[1]
9/23	Lock-In	SS-O(DC)	4.97 (+7%)[3]	.09 (+13%)	146 (-25%)[3]

Table VI
Sample 1-13-47

Date	Data Source	Magnetic Preparation	W(um)	L/H	$4\pi M_s$
	Manuf.[1]	Unknown[1]	7.45	.17	135
9/27	Microscope[2]	Unknown	7.8 (+5%)[1]		
9/27	Microvolt Meter[7]	SS-SO(AC)[6]	4.76 (-36%)		

Table VII
Sample 1-9-3 (Double-sided)

Date	Data Source	Magnetic Preparation	W(um)	L/H	$4\pi M_s$(G)
	Manuf.[1]	Unknown[1]	7.7	.19	179
9/27	Microscope[2]	Last State[2]	7.15 (-7%)[1]		
9/23	Microvoltmeter[5]	SS-O(DC)[4]	5.73 (-26%)	.13 (-32%)	
9/23	Lock-In	SS-O(DC)	5.71 (-26%)[3]	.13 (-32%)	87 (-51%)
9/27	Microvoltmeter[5] & Lock-In	SS-SO(AC)[6]	4.56 (-41%)	.09 (-53%)	103 (-42%)[7]
9/27	Microvoltmeter	SS-SO(AC)	4.60 (-40%)		

Table VIII
Sample 1-9-3 (Single-sided)

Date	Data Source	Magnetic Preparation	W(um)	L/H	$4\pi M_s$(G)
9/27	Microscope[2]	Last State[2]	7.2 (-6%)[1]	.19	
9/27	Microvoltmeter[5]	SS-SO(DC)[3]	4.67 (-39%)		
9/27	Microvoltmeter	SS-SO(DC)	4.16 (-46%)		
9/27	Microvoltmeter	SS-SO(DC)	5.14 (-33%)		
9/27	Microvoltmeter[5] Lock-In	SS-SO(AC)	5.24 (-32%)	.11 (-42%)	150[3] (-16%)

Table IX
Sample 7-1-77 #2

Date	Data Source	Magnetic Preparation	W(um)	L/H	$4\pi M_s$(G)
	Manufacturer[1]	Unknown[1]	2.0	.05	832
9/26	Microvoltmeter[5]	SS-SO(DC)[3]	1.61 (-20%)[1]	.04 (-20%)	___[8]

Table X
Sample 4-3-77 #1

Date	Data Source	Magnetic Preparation	W(um)	L/H	$4\pi M_s$(G)
	Manufacturer[1]	Unknown[1]	1.8	.04	559
9/26	Microvoltmeter[5]	SS-SO(DC)[3]	1.86 (+3%)[1]	.05 (+25%	___[8]
9/26	Microvoltmeter[5]	SS-SO(DC)	1.76 (-2%)[1]	.04	___[8]

Table XI
Sample 4-3-77 #2

Date	Data Source	Magnetic Preparation	W(um)	L/H	$4\pi M_s$(G)
	Manufacturer[1]	Unknown[1]	1.5	.03	555
9/26	Microvoltmeter[5]	SS-SO(DC)[3]	1.86 (+19%)[1]		___[8]

Table XII
Sample 6-20-12

Date	Data Source	Magnetic Preparation	W(um)	L/H	$4\pi M_s$(G)
	Manufacturer[1]	Unknown[1]	2.10	0.14	493
9/22	Microscope[2]	SS-SO(DC)[3]	2.2 (+5%)[1]		
9/26	Microvoltmeter[5] Lock-In	SS-SO(DC)	2.22 (+6%)[1]	0.11 (-21%)	563 (+14%)[9]
9/26	Lock-In	SS-SO(DC)	2.10[10]		499 (+1%)[11]

Table XIII
Sample 6-20-11

Date	Data Source	Magnetic Preparation	W(um)	L/H	$4\pi M_s$(G)
	Manufacturer[1]	Unknown[1]	1.93	0.09	548
9/26	Microvoltmeter	SS-SO(DC)	2.23 (+16%)[1]	0.12 (+33%)	883 (+61%)[12]
9/26	Lock-In[8]	SS-SO(DC)	1.93[10]		728 (+33%)[13]

Table XIV
Sample 4-5-77 #3

Date	Data Source	Magnetic Preparation	W(um)	$4\pi M_s$(G)
	Manufacturer[1]	Unknown[1]	1.5	54
9/22	Microscope[2]	Last State[2]	1.6 (+7%)[1]	
9/13	Lock-In[4]	SS-0(DC)[4]	1.83 (+22%)[3]	___[8]
9/13	Lock-In	SS-0(DC)	1.83 (+22%)[3]	
9/14	Lock-In	SS-0(DC)	1.80 (+20%)[3]	
9/15	Lock-In	SS-0(DC)	1.86 (+24%)[3]	

Table XV
W Versus AC Field for Sample 3-18-16

AC Field (Oe)	Lock-In Amplifier[1] Signal-only Mode	Phase Lock[2]
	W(um)	W(um)
8	4.00	4.00
12	3.96	4.00
15	3.98	3.98
18	4.00	3.93
21	4.00	3.98
24	3.98	3.98
28	4.01	4.00
35	4.04	4.03
42	4.08	4.08

Notes:

1. The Lock-In Amplifier was used as a wide-band signal voltmeter with the spatial-filter.
2. Derivative detection using the Lock-In Amplifier was used in conjunction with the spatial filter.

Magnetic Preparation

1. Unknown: It is not known whether the manufacturer used any type of magnetic preconditioning of the sample before taking measurements.

2. Last State: The sample was used as defined by its last magnetic state. Through out the study stripewidth was assumed to be a constant material parometer that would return to some average valuc after a magnetic disturbance.

3. SS-SO(DC): This preparation technique used the coils C1 and saturated the sample slowly to 230 Oe then slowly back to zero DC field.

4. SS-0(DC): The coils C1 were powered to 230 Oe by the NJE DC power supply, then the power was switched off. It was assumed the stripewidth would assume some repeatable average.

5. Magnet: A 1000 Oe permanent magnet was brought near the sample then removed.

6. SS-SO(AC): The coils C2 were powered to 100 Oe with a 100 Hz AC signal. The current gain was slowly turned up to maximum, then slowly turned down.

Data Source

1. The manufacturer in all cases used optical techniques to determine H (not listed), W, and $4\pi M_s$. The manufacturer's data was available for each sample through the Air Force Avionics Lab, Electronics Resource Branch, Wright-Patterson Air Force Base, Ohio.

2. A Zeiss microscope available late in the study with a poloroid photograph attachment was used. At least two measurements of the photographed stripewidth were made and the results averaged. Accuracy is estimated at no better than 2%, because of the small number of stripewidths considered and because a variation in stripewidth of 0 to 1 um (found in several samples) on a mean 4.0 um stripewidth sample yields a 2% error.

3. Photographed with unknown equipment under contract number AFAL F-33615-77-C-1002.

4. The Lock-In amplifier, with spatial filtering described in the apparatus section of this study, used for both W and $4\pi M_s$.

5. Microvoltmeter and Lock-In: Spatial filtering with the Hewlett-Packard microvoltmeter used to determine the peak response for W and the Lock-In amplifier used for the determination of $4\pi M_s$. The AC field in coils C2 for the AC signal generation were as specified by the note in the $4\pi M_s$ column.

Figure 16. Notes for the column "Data Source" in Tables IV to XV

6. Diffraction: A photograph of the diffraction pattern was obtained and W obtained from it as described in the apparatus section of this study.

7. Microvoltmeter: The microvoltmeter and spatial filter were used together. The Lock-In amplifier was not used.

8. The Lock-In Amplifier was used in conjunction with the spatial filter with the manufacturer's W in an attempt to find the sources of discrepancy.

Figure 17. Notes for the column "Data Source" in Tables IV to XV

W, $4\pi M_S$

1. The percent figure in parenthesis refers to the deviation from manufacturer's data with sign indicating the direction.
2. Not measured.
3. AC field in coils C2 was 8 Oe.
4. AC field in coils C2 was 28 Oe.
5. AC field in coils C2 was 5 Oe.
6. AC field in coils C2 was 21 Oe.
7. AC field in coils C2 was 2 Oe.
8. $4\pi M_S$ could not be measured because the spatial filter could not be positioned close enough to the stage.
9. The signal could not be observed without a very large AC field (approximately 40 Oe). The total field HA was the RMS AC field plus the DC field.
10. Manufacturer's data used for $4\pi M_S$ study.
11. Very large AC field required. Total HA, 168 Oe: 68 Oe RMS AC + 100 Oe DC. Unable to duplicate with any other sample.
12. Very large AC field required. Total HA, 244 Oe: 56 Oe RMS AC + 188 Oe DC.
13. Very large AC field required. Total HA, 219 Oe: 59 Oe RMS AC + 160 Oe DC.

Figure 18. Notes on the columns, W and $4\pi M_S$ from Table IV to XV

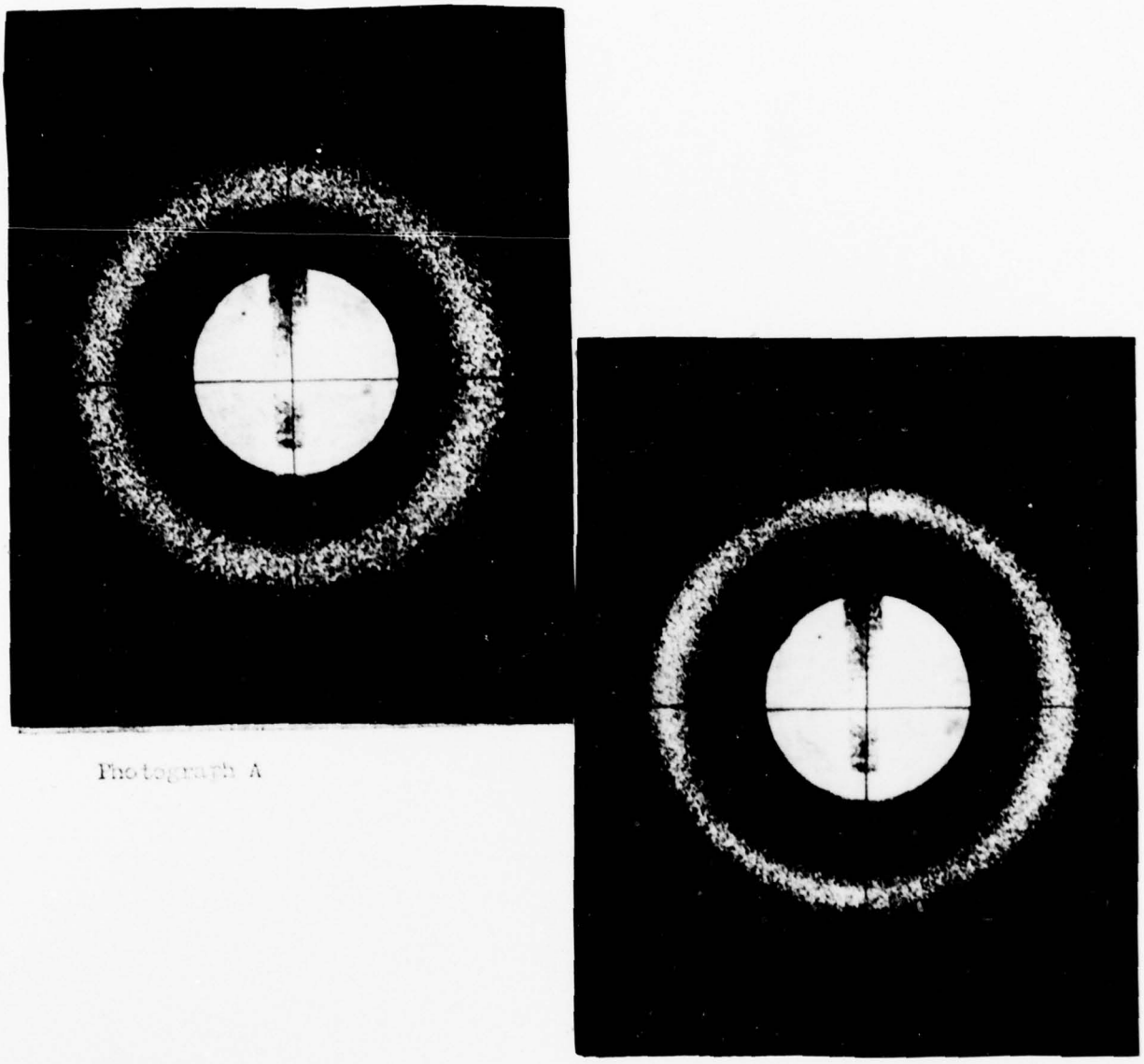

Photograph A

Photograph B

Figure 19. Polaroid Diffraction Photographs of Sample T15696. Picture A Shows the Pattern After DC Saturation and the Field Subsequently Abruptly Removed. Picture B Shows the Pattern with a 2 Oe AC Field.

VI. Conclusions and Recommendations

Conclusions

This study did not confirm validity of the spatial filtering technique for the static characterization of magnetic bubble films with a stripewidth of 4 to 6 um. An examination of Tables V to XIV show that out of 20 trials using the spatial filtering apparatus for the measurement of W, only 3 were within 1 percent of the manufacturer's specifications, and these 3 were for one film, 3-18-16, of Table V. Of the 20 trials, 12 deviated by less than 10 percent and the remainder deviated by a maximum of 41 percent (Table VII). The L/H value was computed for 11 trials and only 2 were within 10 percent of the manufacturer's data. The $4\pi M_s$ value was computed for 9 trials and only 1 trial is within 10 percent. The other measurements of $4\pi M_s$ for these 4 to 7 um films show deviations of up to -51 percent (Table VII). Four of the measurements for $4\pi M_s$ were greater than the manufacturer's optical detection and five were lower.

This study was also inconclusive in extending the spatial filtering technique to 1 to 3 um stripewidth films. Of 12 trials to measure W for these films none were within 1 percent and only 3 were within 5 percent of manufacturer's data, as shown by the data of Tables VI to XI. Only 2 of the 12 trials were less than manufacturer's W, the other trials averaged 14 percent higher. The L/H value was com-

puted for 5 trials and ranged from -20 percent (Table VI) to to +33 percent (Table X). Because the spatial filter could not be placed close enough to the film to measure the second order diffraction angle only two 1 to 3 um films were measured for $4\pi M_s$. The $4\pi M_s$ values of Table IX and X were obtained only with greater than 40 Oe AC fields, and range from +1 percent to +61 percent of the manufacturer's results.

This study did not find a pre-conditioning technique that yielded results for W, L, or $4\pi M_s$ within 10 percent of the manufacturer's data for all films tested. It was initially assumed that after the removal of a saturating magnetic disturbance the films should return to some characteristic condition. Only sample 3-18-16 was believed to have a coercive field greater than 1 G, and even for this film it was believed that the large number of stripewidths covered by laser beam (approximately 125) would negate any effects of localized coercivity due to magnetic or physical defects. The descriptions of the magnetic preparations tried are presented in Figure 15. Very late in the study Henry published a pre-conditioning technique that used an electronically controlled saturating sine wave with a 10 second period (Ref 12:1529). Unfortunately equipment was not available to produce this electronically controlled saturating wave for this experiment. The results of Tables IV to XIV for a manually controlled saturating sine wave, or a manually controlled saturating DC field show that the average stripewidth is a function of the pre-conditioning technique.

This study found no difference in the technique used to measure the maximum photodetector output. From examination of Tables IV to XV it can be seen that the errors are in no particular pattern nor did the Lock-In amplifier prove to be more accurate. For fields below 8 Oe it is believed that the microvoltmeter may provide a more accurate determination based on the results of Figure 19. Figure 19 shows that when a 2 Oe AC field is applied to a sample after a saturating magnetic disturbance the mean radius of the diffraction pattern is increased. This means that the average stripewidth has decreased under the influence of the applied field. Above 8 Oe, the stripewidth changes very little from 8 Oe to 42 Oe as can be seen from Table XV. From Table XV it can be seen also that there is little difference in the technique used to measure the maximum photodetector output. For $4\pi M_s$ measurements it was found experimentally that derivative detection provided the best means of locating the second order maximum. For the 4 to 7 um films tested it was not possible to locate the second order maximum except using derivative detection as described in the Apparatus section of this thesis.

This study found no difference in single versus double sided 4 to 7 um film as is shown in Tables VII and VIII. The spatial filtering technique yielded similarly low values for the measurement of W for both films. The double-sided film averaged 33 percent low for W while the single-sided film averaged 37 percent low. The results for L/H and $4\pi M_s$

are also similar for both films.

The theoretical part of this study did show that if a $4\pi M_s$ value within 1 percent of actual value is desired for 1 to 3 um films with a Q of 3, this Q dependence must be taken into account. It was confirmed that the industrial practice of assuming high Q, for 4 to 7 um films with a Q of 3, will yield a $4\pi M_s$ value within 1 percent of actual value. The plots of Figures 4 to 8 show this deviation. It is also shown in these plots that as Q decreases below 3 and D/H decreases below 1.5 the uncertainty in $4\pi M_s$, as determined using the Kooy and Enz equations, may increase to a maximum of 34 percent for a Q of 1 and zero field D/H of 0.7.

It was not possible to measure the anisotrophy field in this study because the field produced by the bias coils was insufficient. For a $4\pi M_s$ value of 200 G and a Q of 3, a 600 Oe field would be needed. The coils available for use could only produce a maximum of 300 G. It was originally assumed that a pulsed current high enough to extinguish the Faraday rotation could produce the required anisotropic in-plane field. The coils overheated before the Hk field could be established.

Possible Sources of Discrepancy

The question of why this study produced results that differ significantly from the manufacturers was examined and the following explanations are proposed.

The proper technique for magnetic preparation of the sample was not employed. Henry published, too late for it

to be implemented in this research, his technique for sample preparation (Ref 12:1529) and emphasized the importance of preconditioning. It is believed that not only must the sample be free from gross defects but that the sample must be in a true relaxed state for consistent measurements to be taken using the spatial filtering technique. Henry used a ramped-amplitude, sinusoidol, saturating field with a 10 second ramp period. Unfortunately equipment was not available to produce this type of preconditioning. The techniques used in this study were: 1) a manually ramped DC field, 2) a manually ramped DC field suddenly removed at maximum field, and 3) a manually ramped AC field.

It is possible that the manufacturers' data is not accurate, especially for films with a stripewidth of 1 to 3 um. The manufacturer's data was obtained optically and the resolution of the microscope used to determine W and $4\pi M_s$ could be marginal, making accurate measurements difficult. Also the calibration, accuracy or preconditioning of the sample by the manufacturer is not known. Photographs taken of W using a Zeiss microscope show up to 15 percent difference in stripewidth from the value quoted by the manufacturer as can be seen in Tables IV, V, VI, VII, VIII, XII, XIII and XV. However these photographs were taken without knowing the exact preconditioning technique to which they had been subjected. It may be that 5 to 15 percent is the expected range of difference depending on the preconditioning technique applied. The manufacturers' thickness value

was measured using optical spectroscopy with unknown accuracy. This study used H as determined by the manufacturer.

The experimental apparatus was checked and rechecked for systematic error. No systematic error was found in the maximum as the spatial filter was positioned along optical bench for the determination of W, nor was any systematic error found during the measurement of the field to calculate $4\pi M_s$. The measurement of spatial filter-to-bubble film distance was accomplished at least four times for each trial and the results averaged. The radius of the spatial filter was rechecked and the calibrating technique for the optical bench examined for possible error. None was found.

It may be possible that the passband of the spatial filter is to narrow. From Figure 19 it can be seen that the width of the diffracted beam is approximately 1 cm at 30 cm from the bubble film. It was believed that at 10 cm the diffracted beam was only 2 mm wide and that the 1 mm (.030 in) passband of the spatial filter would accurately locate the mean diffraction angle for both W and $4\pi M_s$ measurements. It was learned from Dr. Henry that he used a wider passband spatial filter such that the signal detected, when the beam was centered in the passband, contained none of the reference signal, rather than a maximum of twice the reference signal as used in this study (Ref 9).

Finally it may be that the films selected had a particularly high coercivity and were magnetically or physically defective. The preconditioning technique is important in

the magnetic relaxation of bubble films, but if the film is magnetically or physically defective it is possible that no preconditioning technique would yield consistent results. Magnetic and physical defects tend to "pin" i.e. to immobilize the stripes and it may be that even 125 periods is not sufficient to average out localized defects.

Recommendations

1. It is recommended that a wider selection of samples be tested using the microvoltmeter to determine the maximum response for W calculations, and that the Lock-In Amplifier be used in conjunction with derivative detection for $4\pi M_s$. It is recommended that 4 to 7 um films be selected and the same preconditioning technique that Henry used be employed (Ref 12:1529).
2. It is recommended that a spatial filter be constructed with a 2 cm passband for a nominal 10 cm spatial filter-bubble film distance. This filter should be used to determine if another type of derivation detection yields better results.
3. Diffraction studies should be done on 1 to 3 um films to determine if there is enough diffracted light in the second order to be detected. Studies should be done to determine why a large AC field provided a signal for sample 6-20-12 and 6-20-11 of Table XII and XIII, respectively.
4. Some method must be found to measure Q, either di-

rectly or indirectly. One possibility is to construct coils large enough to provide a 1500 Oe field which should be sufficient for a Q of 3 assuming a maximum $4\pi M_s$ of 500 G.

AD-A055 687 AIR FORCE INST OF TECH WRIGHT-PATTERSON AFB OHIO SCH--ETC F/G 9/2
THE STATIC CHARACTERIZATION OF MAGNETIC BUBBLE FILMS USING SPAT--ETC(U)
DEC 77 R A MCDONALD

UNCLASSIFIED AFIT/GE/EE/77-27 NL

2 OF 2
AD A055 687

END
DATE FILMED
8-78
DDC

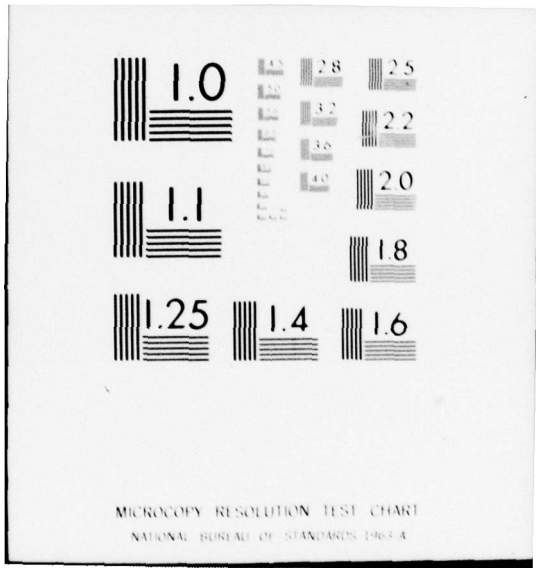
1.0
1.1
1.25
1.4
1.6
1.8
2.0
2.2
2.5
2.8
3.2
3.6
4.0
MICROCOPY RESOLUTION TEST CHART
NATIONAL BUREAU OF STANDARDS 1963-A

Bibliography

1. Ashkin, A. and J. M. Cziedzik. "Interaction of Laser Light with Magnetic Domains." in Magnetic Bubble Technology: Integrated-Circuit Magnetics for Digital Storage and Processing, edited by Hsu Chang. New York: IEEE Press: 1975.

2. Bobeck, A. H. The Development of Bubble Memory Devices. Electro 77 Proceedings, April 19-21, 1977. New York: IEEE, 1977.

3. -----, and E. Della Torre. Magnetic Bubbles. Amsterdam: North Holland Publishing Co., 1975.

4. -----, et al. "An Overview of Magnetic Bubble Domains-Material-Device Interface." in Magnetic Bubble Technology: Integrated-Circuit Magnetics for Digital Storage and Processing, edited by Hsu Chang. New York: IEEE Press: 1975.

5. Buvinger, E. A., and S. E. Cummins. Military Applications of Magnetic Bubble Memories. Electro 77 Proceedings, April 19-21, 1977. New York: IEEE, 1977.

6. Cook, N. H. and E. Pabinowiez. Physical Measurement and Analysis. Reading, Massachusetts: Addison-Wesley Publishing Company, Inc., 1963.

7. Chang, H. ed., Magnetic Bubble Technology: Integrated-Circuit Magnetics for Digital Storage and Processing. New York: IEEE Press, 1975.

8. Haskal, H. M. "Polarization and Efficiency in Magnetic Holography." IEEE Transactions on Magnetics, 6:542-545 (September, 1970).

9. Henry, R. D. Rockwell International, Electronics Research Division, Anaheim, California 92803. Telephone conversation 30 September, 1977.

10. -----. "Bubble Material Characterization Using Spatial Filtering." Materials Research Bulletin, 11:1285-1293 (October 1976).

11. -----. "Bubble Materials Characterization Using Spatial Filtering Techniques." Unpublished preprint of paper presented at the International Magnetics Conference, June 1977, in Los Angeles, California.

12. -----. "Bubble Material Characterization Using Spatial Filtering Techniques." IEEE Transactions on Magnetics, 13:1527-1531 (September 1977).

13. Instruction Manual Precision Lock-In Amplifier Model HR-8. Princeton, New Jersey: Princeton Applied Research Corporation, 1965.

14. Kestigian, M., et al. Magnetic IPE Crystalline Films For Small Bubble Diameter Cylindrical-Domain Memory Applications. Prepared for the Air Force Office of Scientific Research, Bolling Air Force Base, Washington D. C., by Sperry Research Center, 100 North Road, Sudbury, Ma. July, 1977.

15. Kooy, C. and U. Enz. "Experimental and Theoretical Study of the Domain Configuration in Thin Layers of $BaFe_{12}O_{19}$." Philips Research Reports, 15:7-29 (February 1960).

16. Maartense, I., C. W. Searle, and M. G. Mier. "Bubble Film Characterization by AC Susceptibility Measurements." To be published. Maartense and Searle are with the Department of Physics, University of Manitoba, Winnipeg, Canada. Mier is with the Electronics Research Branch, Electronic Technology Division, Air Force Avionics Laboratory, Wright-Patterson Air Force Base, Ohio, 45433.

17. Mezrich, R. S. "Reconstruction Effects in Magnetic Holography." IEEE Transactions on Magnetics, 6:537-541 (September 1970).

18. Model 124B Helium-Neon Gas Laser Instruction Manual. Mountain View, California: Spectra-Physics, Inc. 1969.

19. Searle, C. W. Department of Physics, University of Manitoba, Winnipeg, Canada. Private Communication, 30 September 1977.

20. Shaw, R. W., R. M. Sandfort, and J. W. Moody. Characterization Techniques Study Report Magnetic Bubble Materials. ARPA Order Nr. 1999. Advanced Research Projects Agency, Department of Defense, Washington, D. C. AD748426.

21. -----, et al. "Determination of Magnetic Bubble Film Parameters from Strip Domain Measurements." Journal of Applied Physics. 44:2346-2349 (May 1973).

22. Thiele, A. A. "The Theory of Cylindrical Magnetic Domains." The Bell System Technical Journal, 48:3287-3335 (December).

23. -----. "Device Implications of the Theory of Cylindrical Magnet Domains." in Magnetic Bubble Technology: Integrated-Circuit Magnetics for Digital Storage and Processing, edited by Hsu Chang. New York: IEEE Press, 1975.

Appendix A

Appendix A contains the list of equipment used and the specifications for the components of Figure 10.

Appendix A

List of Equipment

Item	Manufacturer	Model	Serial
HeNe Laser	Spectra Physics	124 A	3275 825
HeNe Laser	Spectra Physics	135	3311 601
Filter .6328um	Oriel Co.	#6328A/30#8	
Lens A, 10 cm focal length 63mm Dia	Ealing Optics	#A23-9228	
Lens B, 5 cm focal length	Ealing Optics	#A23-9202	
Photo detector, PIN Silicon Diode with Op-Amp	United Detector Technology, Inc.	UT505	
Lock-In Amplifier with Type-C pre-amplifier	Princeton Applied Research	HR-8	1249
DC Power Supply	NJE Corp	CR60-9	X130-3
Oscillator	Hewlett-Packard	200CD	#75
Microvoltmeter	Hewlett-Packard	425A	426 06577
Magnetic field strength with	Bell Gaussmeter	615	104599

Item	Manufacturer	Model	Serial
10X probe	Bell Gaussmeter	T610-352	104812
Oscilloscope	Tektronix	Type 585A	011432
Type 82 Plug-In Unit	Tektronix	Type 82	006644
Optical Bench	Gaertner Scientific Corp.		
Camera	Graphex	Crown Graphic	
Multimeter	Fluke	8100 A	1817
Vernier Caliper	L. S. Starrett Co.	#122	

R1, resistor, 2 ohm, 40 watts

R2, resistor, 100 kohm, ½ watt

C1, 4 in I.D. Coils, 300 turns #18 AWG Copper

C2, 1½ in I.D. Coils, 200 turns #20 AWG Copper

D1, Diodes (4), 1N4002

T1, Transformer, 110VAC/12VAC, Stancor, p 3020

Note: R1, R2, C1, C2, D1, and T1 refer to Figure 10.

Appendix B

The Fortran computer program of the Kooy and Enz equation used to generate Tables of D/H versus L/H for M/M_S = 0.0, and M/M_S = 0.5 is listed. Sample values from the tables are listed.

```
PROGRAM BOB4       74/74   OPT=1                          FTN 4.5+414

      PROGRAM BOB4(INPUT,OUTPUT,PLOT,TAPE1)
C
C
C     A PROGRAM TO TABULATE AND PLOT THE THE K AND EQ. (10)
C
C     PERIOD IS D,THICKNESS IS H, MAGNETIZATION IS M
C     CHARACTERISTIC LENGTH IS L
C     THE PROGRAM COMPUTES L/H AS A FCN OF D/H,Q AND M/MS
C
C     PLOT 1 IS M/MS=0,D/H= 0.5 TO 1.5
C     PLOT 2 IS M/MS=0.5,D/H=0.5 TO 1.5
C     PLOT 3 IS M/MS=0,D/H=1.5 TO 2.5
C     PLOT 4 IS M/MS=0.5,D/H= 1.5 TO 2.5
C     PLOT 5 IS M/MS= 0.,D/H = 2.5 TO 3.5
C     PLOT 6 IS M/MS = 0.5,D/H= 2.5 TO 3.5
C
      DIMENSION STORCO(8),X(103),Y1(103),Y2(103),Y3(103),Y4(103)
      DIMENSION STOR(10)
      REAL M,LOVH
      INTEGER CO,STORCO
      DATA PI/3.1415926 54/
C     RANGE OF Q IS 1-7,1000
C
C     RANGE OF M/MS IS 0.0 AND 0.5 THE SF PTS
C
C      ALL DIM ARE CGS
      BB=0.5
      YST=0.0
      DO 20 II=1,3
      M=0.0
      DO 10 I=1,2
      B=BB
      PRINT 14,M
14    FORMAT (*1*,10X,*TABLE OF D/H VS L/H
     1FOR Q EQ 1 TO 7 INCLUSIVE AND Q EQ 1000*,
     210X,*M/MS=*,E10.4/)
      PRINT 15
15    FORMAT(19X,*Q=1*,12X,*Q=2*,12X,*Q=3*,
     312X,*Q=4*,12X,*Q=5*,12X,*Q=6*,12X,
     4*Q=7*,12X,*Q=1000*)
      PRINT 16
16    FORMAT(3X,*D/H*,11X,8(*-L/H*,11X)/
     12X,9(10(*-*),5X)/)
      J2=0
```

```
      DO 11 J=1,101
      IF(J2.EQ.53) PRINT 14,M
      IF(J2.EQ.53) PRINT 15
      IF(J2.EQ.53) PRINT 16
      IF(J2.EQ.53) J2=1
      DO 12 K=1,8
      J1=K
      Q=K
      IF(Q.EQ.8) Q=1000.
      U=1.+1./Q
      URT=SQRT(U)
      CALL SUM(PI,M,URT,B,SOM,CO)
      STORCO(J1)=CO

      LOVH=(2.*B*B*SOM)/((1.+URT)*PI**3)
      IF(Q.GT.0.99.AND.Q.LT.1.01) Y1(J)=LOVH
      IF(Q.GT.2.99.AND.Q.LT.3.01) Y2(J)=LOVH
      IF(Q.GT.4.99.AND.Q.LT.5.01) Y3(J)=LOVH
      IF(Q.GT.999.99.AND.Q.LT.1000.01) Y4(J)=LOVH
      STOR(1)=B
      STOR(J1+1)=LOVH
12    CONTINUE
      J2=J2+1
      PRINT 13,(STOR(IA),IA=1,9)
13    FORMAT(1X,F9.2,5X,8(F8.5,7X))
      X(J)=B
      WRITE(1,25) X(J),Y1(J),Y2(J),Y3(J),Y4(J)
25    FORMAT(1X,5(G12.6,4X))
      B=B+0.01
11    CONTINUE
      CALL PLOT (0.0,-3.0,-3)
      CALL PLOT(1.0,1.0,-3)
      X(102)=BB
      X(103)=.20
      Y2(102)=Y3(102)=Y4(102)=Y1(102)=YST
      Y2(103)=Y3(103)=Y4(103)=Y1(103)=0.015
      CALL AXIS(0.0,0.0,3HD/H,-3,5.0,0.0,X(102),X(103))
      CALL AXIS(0.0,0.0,3HL/H,3,9.0,90.0,Y1(102),Y1(103))
      CALL LINE(X,Y1,101,1,5,2)
      CALL LINE(X,Y2,101,1,6,3)
      CALL LINE(X,Y3,101,1,7,4)
      CALL LINE(X,Y4,101,1,8,5)
```

```
      CALL SYMBOL(1.,9.,.14,2,0.,-1)
      CALL SYMBOL(1.5,9.,.14,3HQ=1,0.,3)
      CALL SYMBOL(1.,8.5,.14,3,0.,-1)
      CALL SYMBOL(1.5,8.5,.14,3HQ=3,0.,3)
      CALL SYMBOL(1.,8.0,.14,4,0.,-1)
      CALL SYMBOL(1.5,8.0,.14,3HQ=5,0.,3)
      CALL SYMBOL(1.,7.5,.14,5,0.,-1)
      CALL SYMBOL(1.5,7.5,.14,6HQ=1000,0.,6)
      CALL SYMBOL(3.0,0.5,.14,2HM=,0.,2)
      CALL NUMBER(3.5,0.5,.14,M,0.,1)
      CALL PLOT(10.0,0.0,-3)
      M=M+0.5
   10 CONTINUE
      BB=BB+1.0
      YST=YST+0.09
   20 CONTINUE
      CALL PLOTE(N)
      STOP
      END
```

SUBROUTINE SUM 74/74 OPT=1

```
      SUBROUTINE SUM(PI,M,URT,B,SOM,CO)
      REAL PI,M,URT,TERM,ARGA,ARGSIN,SINARG
      REAL EXPARG,PLAC,Z,SOM
      INTEGER II,CO,CO1,CO2,CO3
      DIMENSION PLAC(4)
      DATA Z/0.0/
      DATA (PLAC(IA),IA=1,4)/4(0.0)/
      SOM=0.0
      II=1000
      ARGA=1.+M
      DO 30 I=1,II
      CO=I
      ARGSIN=ARGA*CO*PI/2.
      SINARG=SIN(ARGSIN)
      ARGEXP=-2.*PI*CO*URT/B
      IF(ARGEXP.LT.-600.) ARGEXP=-600.
      EXPARG=EXP(ARGEXP)
      TERM=(SINARG*SINARG)*(1.-((1.+2.*PI
     1*CO*URT/B)*EXPARG))/CO**3
      SOM=SOM+TERM
      CO1=CO-1
      CO2=MOD(CO1,4)
      CO3=CO2+1
      PLAC(CO2+1)=SOM
      IF(CO3.EQ.4) 31,30
   31 Z=ABS((PLAC(1)+PLAC(2))-(PLAC(3)
     1+PLAC(4)))
      IF(Z.LT.1.E-6) RETURN
   30 CONTINUE
      RETURN
      END
```

Table XVI

D/H vs. L/H, $M/M_s = 0.0$

D/H	Q=1 -L/H	Q=3 -L/H	Q=5 -L/H	Q=1000 -L/H
1.50	.06212	.06773	.06891	.07061
1.51	.06291	.06855	.06973	.07142
1.52	.06370	.06937	.07056	.07223
1.53	.06450	.07020	.07138	.07305
1.54	.06531	.07103	.07221	.07387
1.55	.06611	.07186	.07304	.07469
1.56	.06693	.07269	.07387	.07551
1.57	.06774	.07353	.07471	.07634
1.58	.06856	.07437	.07555	.07716
1.59	.06938	.07521	.07638	.07799
1.60	.07020	.07605	.07723	.07882
1.61	.07103	.07690	.07807	.07965
1.62	.07186	.07775	.07891	.08048
1.63	.07270	.07860	.07976	.08131
1.64	.07354	.07945	.08061	.08214
1.65	.07438	.08030	.08146	.08298
1.66	.07522	.08116	.08231	.08381
1.67	.07607	.08202	.08316	.08465
1.68	.07692	.08288	.08402	.08548
1.69	.07777	.08374	.08487	.08632
1.70	.07863	.08461	.08573	.08716
1.71	.07949	.08548	.08659	.08800
1.72	.08035	.08634	.08745	.08884
1.73	.08122	.08721	.08832	.08968
1.74	.08209	.08808	.08918	.09053
1.75	.08296	.08896	.09005	.09137
1.76	.08383	.08983	.09091	.09221
1.77	.08471	.09071	.09178	.09306
1.78	.08559	.09159	.09265	.09390
1.79	.08647	.09247	.09352	.09475
1.80	.08736	.09335	.09439	.09560

1.81	.08825	.09423	.09526	.09644
1.82	.08914	.09511	.09614	.09729
1.83	.09003	.09600	.09701	.09814
1.84	.09093	.09689	.09789	.09899
1.85	.09182	.09777	.09876	.09984
1.86	.09272	.09866	.09964	.10069
1.87	.09363	.09955	.10052	.10154
1.88	.09453	.10044	.10140	.10238
1.89	.09544	.10134	.10228	.10323
1.90	.09635	.10223	.10316	.10409
1.91	.09726	.10312	.10404	.10494
1.92	.09818	.10402	.10492	.10579
1.93	.09909	.10492	.10580	.10664
1.94	.10001	.10581	.10668	.10749
1.95	.10093	.10671	.10757	.10834
1.96	.10185	.10761	.10845	.10919
1.97	.10278	.10851	.10934	.11004
1.98	.10371	.10941	.11022	.11089
1.99	.10463	.11031	.11111	.11174
2.00	.10556	.11122	.11199	.11259
2.01	.10650	.11212	.11288	.11344
2.02	.10743	.11302	.11377	.11429

Table XVII

D/H vs. L/H, $M/M_S = 0.5$

D/H	Q=1 -L/H	Q=3 -L/H	Q=5 -L/H	Q=1000 -L/H
1.50	.03896	.04271	.04355	.04482
1.51	.03946	.04324	.04408	.04535
1.52	.03997	.04377	.04462	.04589
1.53	.04047	.04430	.04515	.04643
1.54	.04098	.04484	.04569	.04696
1.55	.04150	.04538	.04623	.04750
1.56	.04201	.04591	.04677	.04804
1.57	.04253	.04646	.04732	.04859
1.58	.04305	.04700	.04786	.04913
1.59	.04357	.04754	.04841	.04968
1.60	.04409	.04809	.04896	.05022
1.61	.04462	.04864	.04951	.05077
1.62	.04515	.04919	.05006	.05132
1.63	.04568	.04974	.05061	.05188
1.64	.04621	.05030	.05117	.05243
1.65	.04675	.05085	.05172	.05298
1.66	.04729	.05141	.05228	.05354
1.67	.04783	.05197	.05284	.05409
1.68	.04837	.05253	.05340	.05465
1.69	.04892	.05309	.05397	.05521
1.70	.04946	.05366	.05453	.05577
1.71	.05001	.05422	.05510	.05633
1.72	.05057	.05479	.05567	.05690
1.73	.05112	.05536	.05623	.05746
1.74	.05167	.05593	.05680	.05802
1.75	.05223	.05651	.05738	.05859
1.76	.05279	.05708	.05795	.05916
1.77	.05336	.05765	.05852	.05973
1.78	.05392	.05823	.05910	.06030
1.79	.05449	.05881	.05968	.06087
1.80	.05505	.05939	.06026	.06144

1.81	.05552	.05997	.06084	.06201
1.82	.05620	.06056	.06142	.06258
1.83	.05677	.06114	.06200	.06316
1.84	.05735	.06172	.06258	.06373
1.85	.05793	.06231	.06317	.06431
1.86	.05951	.06290	.06375	.06488
1.87	.05909	.06349	.06434	.06546
1.88	.05967	.06408	.06493	.06604
1.89	.06026	.06467	.06552	.06662
1.90	.06084	.06527	.06611	.06720
1.91	.06143	.06586	.06670	.06778
1.92	.06202	.06646	.06729	.06836
1.93	.06262	.06705	.06788	.06894
1.94	.06321	.06765	.06848	.06952
1.95	.06381	.06825	.06907	.07011
1.96	.06441	.06885	.06967	.07069
1.97	.06501	.06945	.07026	.07128
1.98	.06561	.07005	.07086	.07186
1.99	.06621	.07066	.07146	.07245
2.00	.06681	.07126	.07206	.07303
2.01	.06742	.07187	.07266	.07362
2.02	.06803	.07247	.07326	.07421

Appendix C

The Fortran computer program of the Kooy and Enz equation used to generate $HA/4\pi M_S$ versus D/H at $M/M_S = 0.5$ is listed. Sample values from the table are also listed.

```
      PROGRAM 303(INPUT,OUTPUT,TAPE2)
C
C     TABLE OF M*Z*PI**2 AS A FUNCTION
C     OF D/H FROM K AND L SQ(S)
C
C     D/H IS THE REDUCED PERIOD
C
      REAL M
      DIMENSION HOVMS(500,7)
      DIMENSION ERROR(500,5)
      DIMENSION TERM(500,5)
      PI=3.14159265
      B=0.5
C     B IS THE START OF THE TABLE
C
      L=450
C
C     L IS THE NUMBER OF TABLE ENTRIES
C
      M=0.5
C     M IS M/MS
      DO 10 I=1,L
      DO 11 II=1,5
      IF (II.EQ.1) Q=1.
      IF (II.EQ.2) Q=3.
      IF(II.EQ.3) Q=5.
      IF(II.EQ.4) Q=1000.
      URT=SQRT(1.+1./Q)
      CALL SUM1(PI,URT,B,M,SUM,Z,T)
      ERROR(I,1)=B
      TERM(I,1)=T
      ERROR(I,II+1)=Z
      TERM(I,II+1)=T
      HOVMS(I,II+1)=M*(SUM*B*2.)/(PI*PI*(1.+URT))
   11 CONTINUE
      HOVMS(I,1)=B
      WRITE(2,40) (HOVMS(I,IA),IA=1,5)
   40 FORMAT(1X,5(G12.6,1X))
      B=B+0.01
   10 CONTINUE
      PRINT 12,M
      PRINT 13
      PRINT 14
      DO 20 K=1,L
      PRINT 15,(HOVMS(K,IA),IA=1,5)
      KK=MOD(K,51)
      IF(KK.EQ.50) PRINT 41
      IF(KK.EQ.50) PRINT 14
   20 CONTINUE
      PRINT 22
      DO 23 KA=1,L
      PRINT 24,(ERROR(KA,KB),KB=1,5)
   23 CONTINUE
      PRINT 31
      DO 30 KC=1,L
      PRINT 32,(TERM(KC,KD),KD=1,5)
   30 CONTINUE
```

```
      PROGRAM BOB         74/74   OPT=1                          FTN 4.5+414

                  12    FORMAT(*1*,10X,*TABLE OF HA/4!PI!MS,M/MS IS*,
                       11X,F5.2/)
60                13    FORMAT(5X,*D/H*,4X,4(*HA/4!PI!MS*,4X))
                  14    FORMAT(1+X,*0=1*,11X,*0=3*,11X,*0=5*,11X,*0=1000*/)
                  15    FORMAT(5X,F4.2,3X,4(F8.6,6X))
                  22    FORMAT(*1*,*ERROR TABLE, SEE PROG FOR DEF OF Z*/)
                  24    FORMAT(1X,5(E13.7,3X))
65                31    FORMAT(*1*,*NUMBER OF TERMS TO CONVERGE TO LT 1.E-6*/)
                  32    FORMAT(1X,F5.3,4(F12.2,4X))
                  41    FORMAT (*1*)
                        STOP
                        END
```

```
      SUBROUTINE CUM      74/74   OPT=1                          FTN 4.5+414

   1                    SUBROUTINE CUM(PI,URT,Q,M,SUM,Z,RI)
                        REAL M
                        DIMENSION STOR(4)
                        SUM=0.0
   5                    DO 10 I=1,3000
                        RI=I
                        A=2.*PI*RI*URT/Q
                        IF(A.GT.600.) A=600.
                        SUM=SUM+((SIN(RI*PI*(1.+M)))*(1.-EXP(-A)))/(RI*RI)
  10                    IA=MOD(I,4)
                        IF(IA.EQ.0) IA=4
                        STOR(IA)=SUM
                        Z=ABS((STOR(4)+STOR(3))-(STOR(2)+STOR(1)))
                        IF(Z.LT.1.E-6) RETURN
  15                10  CONTINUE
                        RETURN
                        END
```

Table XVIII

$HA/4\pi M_s$, M/M_s = 0.5

TABLE OF HA/4:PI:MS, M/MS IS .50

D/H	HA/4:PI:MS Q=1	HA/4:PI:MS Q=3	HA/4:PI:MS Q=5	HA/4:PI:MS Q=1000
2.53	.311813	.293378	.291995	.285502
2.54	.311164	.294020	.291347	.285955
2.55	.310510	.294263	.290701	.285338
2.56	.309857	.293619	.290056	.284709
2.57	.309207	.292969	.289413	.284082
2.58	.308553	.292322	.288773	.283457
2.59	.307905	.291678	.288134	.282834
2.60	.307258	.291033	.287496	.282213
2.61	.306611	.290391	.286861	.281594
2.62	.305965	.289750	.286228	.280977
2.63	.305322	.289112	.285595	.280362
2.64	.304679	.288476	.284966	.279749
2.65	.304037	.287840	.284339	.279138
2.66	.303397	.287207	.283712	.278529
2.67	.302757	.286578	.283087	.277922
2.68	.302119	.285945	.282465	.277317
2.69	.301483	.285317	.281844	.276715
2.70	.300847	.284690	.281225	.276113
2.71	.300213	.284063	.280608	.275514
2.72	.299580	.283442	.279993	.274917
2.73	.298948	.282821	.279379	.274321
2.74	.298318	.282201	.278768	.273728
2.75	.297689	.281583	.278158	.273137
2.76	.297061	.280967	.277550	.272548
2.77	.296434	.280352	.276943	.271960
2.78	.295809	.279739	.276339	.271375
2.79	.295184	.279128	.275736	.270791
2.80	.294562	.278519	.275135	.270209
2.81	.293940	.277911	.274536	.269630
2.82	.293320	.277306	.273938	.269052
2.83	.292700	.276700	.273342	.268476
2.84	.292083	.276097	.272749	.267902
2.85	.291465	.275496	.272156	.267330
2.86	.290851	.274896	.271566	.266758
2.87	.290237	.274298	.270977	.266191
2.88	.289624	.273702	.270390	.265624
2.89	.289012	.273108	.269805	.265060
2.90	.288402	.272515	.269222	.264497
2.91	.287793	.271923	.268640	.263936
2.92	.287185	.271334	.268060	.263377
2.93	.286579	.270745	.267482	.262820
2.94	.285974	.270160	.266905	.262264
2.95	.285370	.269575	.266330	.261711
2.96	.284767	.268992	.265757	.261159
2.97	.284165	.268410	.265186	.260609
2.98	.283565	.267831	.264616	.260061
2.99	.282967	.267253	.264048	.259515
3.00	.282369	.266676	.263482	.258970
3.01	.281773	.266101	.262917	.258427
3.02	.281178	.265528	.262355	.257886
3.03	.280584	.264956	.261793	.257347

Vita

Robert Ashley McDonald was born on 21 January 1945 in Jackson, Mississippi. He attended Georgia Institute of Technology, Atlanta, Georgia and Western Kentucky University, Bowling Green, Kentucky, graduating in August 1968 with a Bachelor of Science degree in Industrial Arts Education. After one year of teaching in a high school he entered the Air Force in July 1969 and was commissioned in September 1969. He went to pilot training at Vance Air Force Base, Enid, Oklahoma. In 1971 he was assigned to the 8th Military Airlift Squadron, McChord Air Force Base, Tacoma, Washington, flying the C-141. In February 1975 he attained Flight Examiner status and was assigned to the Standardization Section, 8th MAS. He entered the Air Force Institute of Technology in June 1975. Capt McDonald is married and has one son and one daughter.

Permanent Address: c/o O'Neal Crisp
Route 1
Murphy, North Carolina 28906

This thesis was typed by Mrs. Sharon Maruna

UNCLASSIFIED

SECURITY CLASSIFICATION OF THIS PAGE (When Data Entered)

REPORT DOCUMENTATION PAGE	READ INSTRUCTIONS BEFORE COMPLETING FORM
1. REPORT NUMBER (14) AFIT/GE/EE/77-27	2. GOVT ACCESSION NO. (9) Master's thesis,
4. TITLE (and Subtitle) (6) The Static Characterization of Magnetic Bubble Films Using Spatial Filtering Techniques.	5. TYPE OF REPORT & PERIOD COVERED MS Thesis
	6. PERFORMING ORG. REPORT NUMBER
7. AUTHOR(s) (10) Robert [redacted] McDonald Capt USAF (Ashley)	8. CONTRACT OR GRANT NUMBER(s) (12) 116p
9. PERFORMING ORGANIZATION NAME AND ADDRESS Air Force Institute of Technology (AFIT/EN) Wright-Patterson Air Force Base, Ohio 45433	10. PROGRAM ELEMENT, PROJECT, TASK AREA & WORK UNIT NUMBERS
11. CONTROLLING OFFICE NAME AND ADDRESS Air Force Avionics Laboratory Electronics Research Branch(AFAL/DHR) Wright-Patterson Air Force Base,Ohio 45433 (11)	12. REPORT DATE DEC [redacted]77
	13. NUMBER OF PAGES 114
14. MONITORING AGENCY NAME & ADDRESS(if different from Controlling Office)	15. SECURITY CLASS. (of this report) UNCLAS
	15a. DECLASSIFICATION/DOWNGRADING SCHEDULE

16. DISTRIBUTION STATEMENT (of this Report)

Approved for public release; distribution unlimited.

17. DISTRIBUTION STATEMENT (of the abstract entered in Block 20, if different from Report)

18. SUPPLEMENTARY NOTES

Approved for public release; IAW AFR 190-17

Jerral F. Guess, Captain, USAF
Director of Information

19. KEY WORDS (Continue on reverse side if necessary and identify by block number)

Magnetic Bubble
Magnetic Bubble Material Characterization
Spatial Filtering
Thin-film Garnet

20. ABSTRACT (Continue on reverse side if necessary and identify by block number)

The primary objectives of this study were to confirm the spatial-filtering technique for the static characterization of 4 to 7 um stripewidth magnetic bubble films, and to extend the technique to 1 to 3 um stripewidth films. Another objective was to determine the uncertainty in $4\pi M_s$ values if infinite Q is assumed, when in fact a more modest value ($3<Q<5$) is present.

DD FORM 1 JAN 73 1473 EDITION OF 1 NOV 65 IS OBSOLETE

UNCLASSIFIED

SECURITY CLASSIFICATION OF THIS PAGE (When Data Entered)

012 225

The spatial filtering technique uses the diffraction grating properties of a magnetic bubble film in conjunction with the equations of Kooy and Enz to determine stripewidth, characteristic length, and saturation magnetization. The spatial filter removes unwanted orders from the diffraction pattern. The filtered signal is focused on a photodetector; the first order diffraction angle is measured to find stripewidth and the second order to find saturation magnetization.

The Kooy and Enz equations were computer programmed and tables and plots of characteristic length/thickness and applied field/saturation magnetization prepared. The Quality factor dependence of the equations was investigated, and it is shown that for a Quality factor of 3, and a domain period/thickness of 0.7, a 14 percent uncertainty in the saturation magnetization could be incurred.

The results of the experimental portion of this study do not confirm the validity of the spatial filtering technique for 4 to 7 um films nor extend it to 1 to 3 um stripewidth films. Of 20 trials to measure stripewidth in 4 to 7 um films only 12 were within 10 percent of manufacturer's data. Saturation magnetization values were up to ± 50 percent of manufacturer's data. It is considered possible that lack of suitable magnetic preconditioning before taking measurements contributed to the discrepancy between data obtained from this study and manufacturer's data.